ADVANCES IN ATMOSPHERIC SCIENCES, VOL. 36, SEPTEMBER 2019, 994–1014

• **Original Paper** •

A Review of Atmospheric Electricity Research in China from 2011 to 2018

Xiushu QIE*[1,3,4] and Yijun ZHANG[2,3]

[1]*Key Laboratory of Middle Atmosphere and Global Environment Observation, Institute of Atmospheric Physics, Chinese Academy of Sciences, Beijing* 100029*, China*

[2]*Department of Atmospheric and Oceanic Sciences and Institute of Atmospheric Sciences, Fudan University, Shanghai* 200438*, China*

[3]*Collaborative Innovation Centre on Forecast and Evaluation of Meteorological Disasters, Nanjing University of Information Science and Technology, Nanjing* 210044*, China*

[4]*College of Earth and Planetary Science, University of Chinese Academy of Sciences, Beijing* 100049*, China*

(Received 27 September 2018; revised 15 February 2019; accepted 15 March 2019)

ABSTRACT

Atmospheric electricity research has been conducted actively in China, having profited from the development and application of high temporal and spatial resolution lightning detection and location technologies. This paper reviews the scientific advances made in the field of atmospheric electricity in China from 2011 to 2018, covering the following five aspects: (1) lightning detection and location techniques; (2) discharge processes and parameters associated with rocket-triggered lightning; (3) physical processes in natural lightning and attachment to the ground; (4) lightning activities and charge structure in different thunderstorms; and (5) effects of thunderstorms on the upper atmosphere. In addition, some outstanding questions for future research are outlined.

Key words: atmospheric electricity, lightning, thunderstorm, lightning location techniques

Citation: Qie, X. S., and Y. J, Zhang, 2019: A review of atmospheric electricity research in China from 2011 to 2018. *Adv. Atmos. Sci.*, **36**(9), 994–1014, https://doi.org/10.1007/s00376-019-8195-x.

Article Highlights:

- High temporal and spatial resolution lightning detection and location technologies have been developed and utilized in China.
- Physical processes in natural lightning, tower-initiated and rocket-triggered lightning flashes have been studied actively from 2011 to 2018.
- Lightning activities and charge structure in different thunderstorms and their effects on the upper atmosphere are reviewed.

1. Introduction

In the study of atmospheric electricity, various electrical processes taking place in the atmosphere are considered, usually within a framework of a global electric circuit, in which thunderstorm regions and fair-weather regions, together with the earth and the lower ionosphere, are combined into a distributed electric circuit. A central issue concerning research on atmospheric electricity in China is lightning and its effects in a wide range of aspects. Qie (2012) reviewed the research progress in atmospheric electricity in China during the period 2006–10. In the present paper, the period 2011–18 is reviewed.

Most achievements in the study of atmospheric electricity in the last few years have come from the coordinated research efforts of the "Program on Dynamic, Microphysical and Electrical Processes in Severe Thunderstorms and Lightning Hazards" (Strom973), which was funded as a National Key Basic (973) Research Program by the Ministry of Science and Technology, China. The Storm973 program carried out six major research topics: (1) Coordinated Observation of Lightning and Thunderstorms based on New Detection Techniques; (2) Evolution of Dynamical Processes and Structures of Strong Thunderstorms; (3) Microphysical Characteristics and their Impacts on Electrical Charge Distribution Inside Thunderstorms; (4) Charge Structure and Lightning Development in Severe Thunderstorms; (5) Physics of Lightning Discharge and Hazard Causes; and (6) Lightning Data Assimilation and Forecasting of Thunderstorms and Lightning.

This review paper covers the following five aspects: (1) lightning detection and location techniques; (2) discharge

* Corresponding author: Xiushu QIE
Email: qiex@mail.iap.ac.cn

processes and parameters associated with rocket-triggered lightning; (3) physical processes in natural lightning and attachment to ground; (4) lightning activities and charge structure in different thunderstorms; and (5) effects of thunderstorms on the upper atmosphere. In addition, some outstanding questions for future research are outlined.

2. Lightning detection and location technology

New lightning observational capabilities have been critical in allowing new understanding on the nature of lightning. Besides steady improvements in electronics and signal processing, a major advance for lightning detection has been the advent of the GPS constellation, which provides extremely accurate timing worldwide. These new capabilities have enabled several groups in China to develop the 3D positioning systems for lightning radiation pulses based on the time-of-arrival technique or interferometry techniques.

2.1. *Long baseline lightning locating system and 3D lightning mapping*

In addition to operational cloud-to-ground (CG) lightning location networks covering all of China, several 3D lightning location research systems have been developed and put forward in lightning detection and research. Figure 1 shows the distribution of major research lightning networks in China's mainland. Zhang et al. (2010) developed the first 3D very-high-frequency (VHF) lightning radiation source mapping technique in China, which was first installed in Zhanhua, Shandong Province. It was then moved to Qinghai Province to investigate the lightning characteristics and charge structure associated with plateau thunderstorms. The system is operated at 270 MHz with a 3-dB bandwidth of 6 MHz and processes peak events in a consecutive time window of 50 μs (Li et al., 2017b). Zhang et al. (2015a) estimated the location error for this system using a balloon-borne VHF transmitter. The system showed a horizontal error of 12–48 m and a vertical uncertainty of 20–78 m for radiation sources over the network. A broadband electric field (E-field) location system working at a bandwidth from 1.5 kHz to 10 MHz is installed synchronously (Li et al., 2013).

A multiband 3D lightning location network has been installed in Beijing, referred to as the Beijing Lighting Network (BLNet). BLNet is a regional lightning location network with one data center and sixteen substations. Each station is equipped with fast antenna, used for real-time location, while two systems from slow antenna, magnetic antenna and VHF antenna are selected to be equipped at each station (Wang et al., 2015c, 2016d), covering a bandwidth from very low frequency (VLF) to VHF. According to Srivastava et al. (2017), the average detection efficiency (DE) of BLNet for total flashes is 93.2%, and 73.9% for CG flashes. The location error in the horizontal direction ranges from 52.9 m to 250.0 m, based on high-tower lightning flashes.

A low frequency (LF) E-field Detection Array (LFEDA) is installed in Conghua, Guangdong, aimed at locating the 3D positions of lightning pulse discharge events (Shi et al., 2017). After checking the LFEDA locations for triggered lightning, it was found that LFEDA has an average horizontal location error of 102 m for return strokes (RSs), with the DE for flashes and RSs being 100% and 95%, respectively. Fan et al. (2018c) developed a new 3D location method for the LFEDA, which significantly increased the capability of the system. For a fatal "bolt from the blue", the mean location

Fig. 1. Distribution of major research lightning networks (red stars) and sites of rocket-triggering lightning experiments (blue triangles) in China's mainland.

error for five strokes was 27 m.

Another lightning location network was set up in Chongqing. The lightning sensors in the network detect VLF/LF and VHF sources radiated by lightning (Liu et al., 2018b). The network is composed of 14 lightning sensors. The minimum and maximum distance between two sensors is about 10 km and 100 km. Each sensor records the VLF/LF and VHF signals continuously at sample rates of 5 MHz and 20 MHz, respectively.

In addition, there are several lightning location networks operating in China and it is important to evaluate the detection performance of these systems. Chen et al. (2012) investigated the performance of three lightning location systems (LLSs) in Guangdong Province based on tower lightning and rocket-triggered lightning. The location error, flash DE, stroke DE, and peak current absolute percentage errors are around 710 m, 94%, 60% and 16.3%, respectively, for the Guangdong Power Grid LLS. For the Guangdong–Hong Kong–Macao LLS (GHMLLS), the flash DE, stroke DE, location error are 74%, 96% and 532 m, respectively. However, the GHMLLS-inferred peak currents were found to be about 37% lower than the actual value during 2012–15. The corresponding values for the Earth Networks Total Lightning Network are 77%, 76%, 685 m and 39% (Zhang et al., 2016b).

The performance of the World Wide Lightning Location Network (WWLLN) was evaluated over the Tibetan Plateau and the ocean. Fan et al. (2018a) found that the location accuracy of the WWLLN was around 10 km and the DE was 9.37% for CG and 2.58% for total flashes over the Tibetan Plateau. The DE of the WWLLN increased year by year from 4.3% to 19.1% over the Northwest Pacific from 2005 to 2016 (Pan et al., 2013; Wang et al., 2018b; Zhang et al., 2018b). It was roughly 16.8% in Beijing in 2015 and 2016 (Srivastava et al., 2017).

2.2. *Short baseline 2D interferometry location technology*

Interferometry location technology, which measures the phase difference or time difference of the lightning signals from different antennas with very short baselines, has developed quickly in China. This system is usually composed of a four orthogonal broadband antenna array with baselines from around 10 m to several tens of meters (Dong et al., 2002). Cao et al. (2012) developed the short-baseline 2D LLS with a bandwidth from 125 MHz to 200 MHz to locate lightning discharge processes. Sun et al. (2013) proposed an algorithm using a time delay estimation based on generalized cross correlation together with wavelet transform to reduce the noise interfaces. The location accuracy for the discharge channel was highly improved. The system has been used to map rocket-triggered lightning and natural lightning discharges (Sun et al., 2014a, b, 2015). Figure 2 shows a VHF mapping example for rocket-triggered lightning with comparison to an optical image. It can be seen that the VHF-mapped discharge channel is very well matched to the high-speed video image in the view of the camera, with a bias of less than one Charge Coupled Device (CCD) element view, which is less than 10 m at a distance of 980 m (Sun et al., 2014b). Liu et al. (2018b) conducted an observation of two broadband interferometers that were about 8.15 km apart and obtained 3D lightning location discharge results. The results indicated that the system effectively mapped the lightning radiation sources and were in good agreement with optical images.

3. Discharge processes and parameters associated with rocket-triggered lightning

Rocket-triggered lightning experiments using the rocket-wire technique were conducted continuously in Zhanhua, Shandong (SHATLE) and Conghua, Guangdong (GCOELD). The locations of the two sites are shown on the map in Fig. 1. Some new insights into the lightning process and the corresponding electromagnetic (EM) effects have been obtained, having profited from the ability to detect the discharge current and the simultaneous close EM field and channel luminosity evolution. Figure 3 shows site pictures in Zhanhua and Conghua of the triggered lightning experiments using the rocket trailing wire technique. The triggering facilities and main observation devices are also marked. A schematic view of both the triggering site and main observation site in the Zhanhua

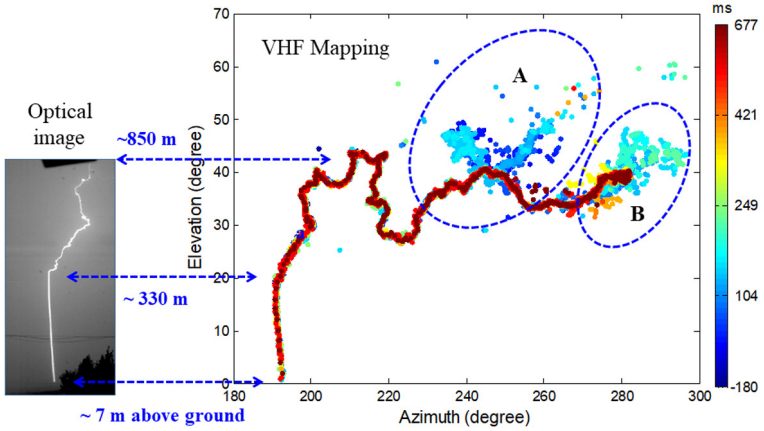

Fig. 2. A triggered lightning discharge channel mapped by a VHF interferometer with comparison to an optical image; modified from Sun et al. (2014b).

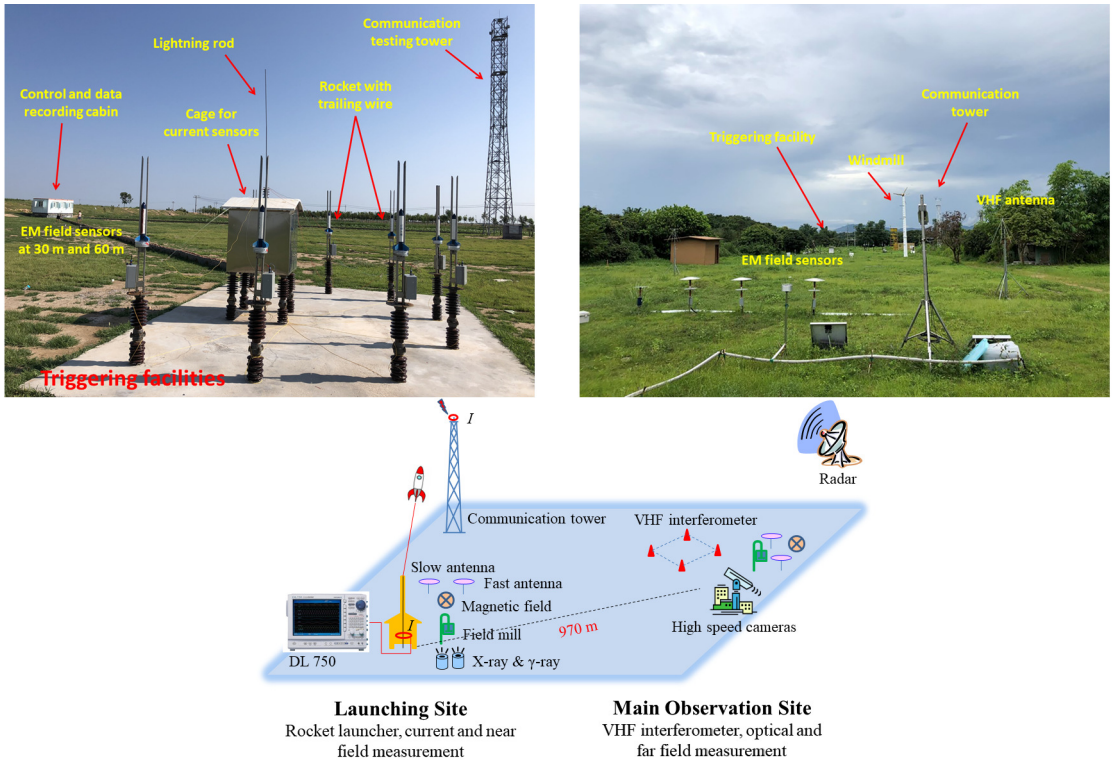

Fig. 3. Installation of rocket-triggering lightning experiment: upper left panel—in SHATLE; upper right panel—in GCOELD; lower panel—schematic view in the Zhanhua experiment.

experiment is also shown in Fig. 3. The primary installation of current and EM field measuring systems are similar at both sites. A schematic view of the Conghua experiment is available in the literature (e.g., Zhang et al., 2016b; Zheng et al., 2017).

3.1. *Upward positive leader*

Rocket-triggered lightning is usually negative in polarity and initiated with an upward positive leader (UPL). The propagating features of UPLs in the initial stage (IS) of triggered lightning were investigated both for SHATLE (Qie et al., 2011, 2012, 2014a, 2017; Wang et al., 2012a; Jiang et al., 2013a) and GCOELD (Zhang et al., 2014c, 2016b; Zheng et al., 2017). The average 2D speed of a UPL was found to be roughly 1.0×10^5 m s^{-1} and showed a tendency to accelerate with height (Jiang et al., 2013a). The peak current for IS pulses ranged from tens of amperes to about 150 A. After a UPL develops to several hundreds of meters high, some impulses can be observed that are superimposed on the initial continuous current (ICC) and the associated E-field (Lu et al., 2014; Fan et al., 2017).

Zhang et al. (2017d) found with a VHF interferometer that precursor pulses appear first during a period of hundreds of milliseconds before the UPL's sustained development in the IS of a triggered lightning discharge. The individual precursor pulses were initiated by weak upward positive breakdown, meters in scale, followed by fast, energetic downward negative breakdown, tens of meters in scale. Their average speed was about 5×10^6 m s^{-1} and 3×10^7 m s^{-1}, respectively.

Lu et al. (2014, 2018) and Fan et al. (2017, 2018d) introduced sensitive LF magnetic sensors into SHATLE in 2013. The UPL propagation was found to be associated with a burst of EM impulses when it entered the in-cloud negative charge center, possibly suggesting a stepped pattern of positive leader propagation even in the cloud (Lu et al., 2014; Zheng et al., 2018). The UPL propagation is active in LF radiation in this period, while it is relatively quiet in the VHF band, implying a possible fundamental change in the progression mechanism of the positive leader. Lu et al. (2016a) classified these magnetic field signals into impulsive and ripple pulses according to their waveform features. At the stage of the impulsive type, the leader channel had a negligible length, so the associated current pulses mainly propagated downward along the high conductivity steel wire into the ground. Based on the above fact, Fan et al. (2018d) simulated the pulse of the impulsive type by using a transmission-line model, suggesting that the pulses are generated by leader current pulses propagating downward along the steel wire. The waveform of impulsive current pulses is changed to ripple pulses after traveling through the high impedance of the prolonging leader channel.

3.2. *Upward negative leader*

Two cases of rare positive lightning flashes were triggered in SHATLE with an upward negative leader (UNL) initiation, but just followed by the ICC stage and without an RS. Figure 4 shows composite UNL images from a high-speed video

camera, together with the UPL images in rocket-triggered lightning. A branched channel structure is apparent for the UNL, while there are no obvious branches for the UPL. Pu et al. (2017) found that the UNL branched shortly after its initiation, and consequently the stepping-caused current pulses became multi-peaked and wider in their waveforms. The negative charge of an individual leader step was nearly an order of magnitude larger than that of the positive counterpart of the triggered lightning. The main negative leader tip propagated at an average speed of 2.1×10^5 m s^{-1}. Two cases of positive lightning flashes without an RS were also triggered in GCOELD (Zheng et al., 2017). The geometric mean (GM) value of the 2D speed of the UNL was 1.79×10^5 m s^{-1}, and the ISs showed much larger currents, charge transfers and action integrals relative to their negative counterpart in GCOELD.

3.3. *Dart leader and bidirectional leader*

Dart leaders usually propagate fast, and a high-speed video camera cannot resolve them well. The VHF/UHF lightning interferometer was upgraded to operate at a continuous recording mode or sequential mode, and is capable of capturing weak radiation signals from lightning, like UPLs, and the discharge channels for downward negative dart leaders can be mapped clearly too (Sun et al., 2014b, 2016). For a triggered negative lightning flash with 16 leader and RS sequences, the dart leader speed was mostly on the order of 10^6–10^7 m s^{-1}. For dart-stepped leaders, it was of 10^5 m s^{-1}.

Bidirectional leader propagation was detected for the first time in triggered lightning discharges by Qie et al. (2017). The bileader initiated almost immediately below a decaying downward leader, which stopped midway before reaching the ground. The average speed of the UPL end was 1.3×10^6 m s^{-1} and 2.2×10^6 m s^{-1} for the two cases, respectively—roughly two times larger than the negative downward leader end. The bidirectional leader might be considered as a polarity-reversed recoil leader with its positive leader end retrogressing along the existing negative channel, and the polarity of the recoil leader here was completely reversed to the traditional one. Zheng et al. (2012) reported an abnormal triggered lightning flash containing two upward propagation processes, with the second upward leader being triggered by a downward aborted leader. They propagated along the same channel but with different polarities and opposite directions.

3.4. *Lightning current characteristics and waveform parameters*

Figure 5 shows an example of the whole current waveform and partial enlarged waveforms of a classical triggered lightning event in Conghua, Guangdong. The flash lasted about 800 ms. The large pulses were produced by 11 RSs, with the peak current from 4 kA to 21 kA. Based on the current and simultaneous close EM field, the discharge processes and corresponding waveform parameters of current pulses were analyzed statistically (Jiang et al., 2011; Wang et al., 2012a; Zhao et al., 2011; Qie et al., 2014a; Zhang et al., 2014c; Zheng et al., 2017). Four categories of current pulses have been found to be associated with triggered flashes: RSs, ICC pulses (ICCPs), M-components superimposed on the continuing current (CC) following the RS, and mixed return stroke- M component (RM) pulses featuring both RS and M-event characteristics. Figure 6 shows the current and corresponding E-field at 60 m produced by these impulsive processes. Differing behavior of the current and E-field can be found between these pulses.

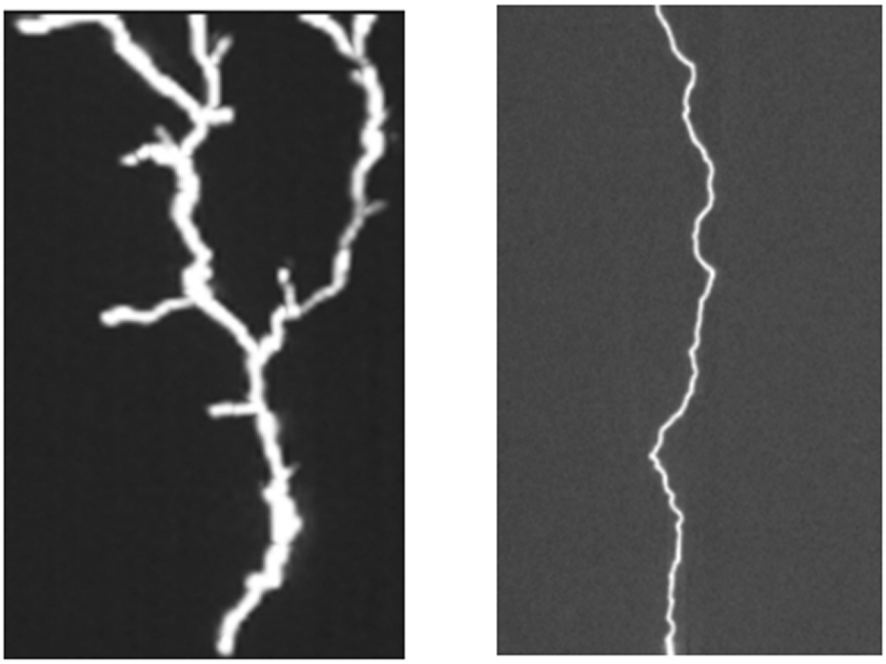

Fig. 4. Composite images of a UNL (left panel) and UPL in rocket-triggered lightning (right panel).

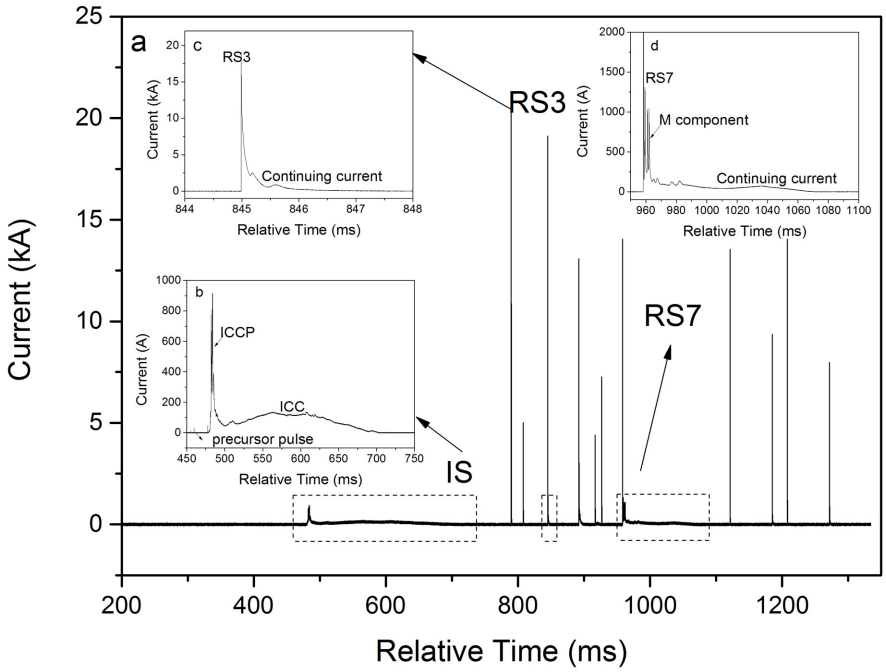

Fig. 5. Example of the current waveform of a classical triggered lightning flash in Conghua, Guangdong: (a) whole current waveform; (b) IS current; (c, d) enlarged current waveforms of the third and seventh RS and the following CCs and M-component.

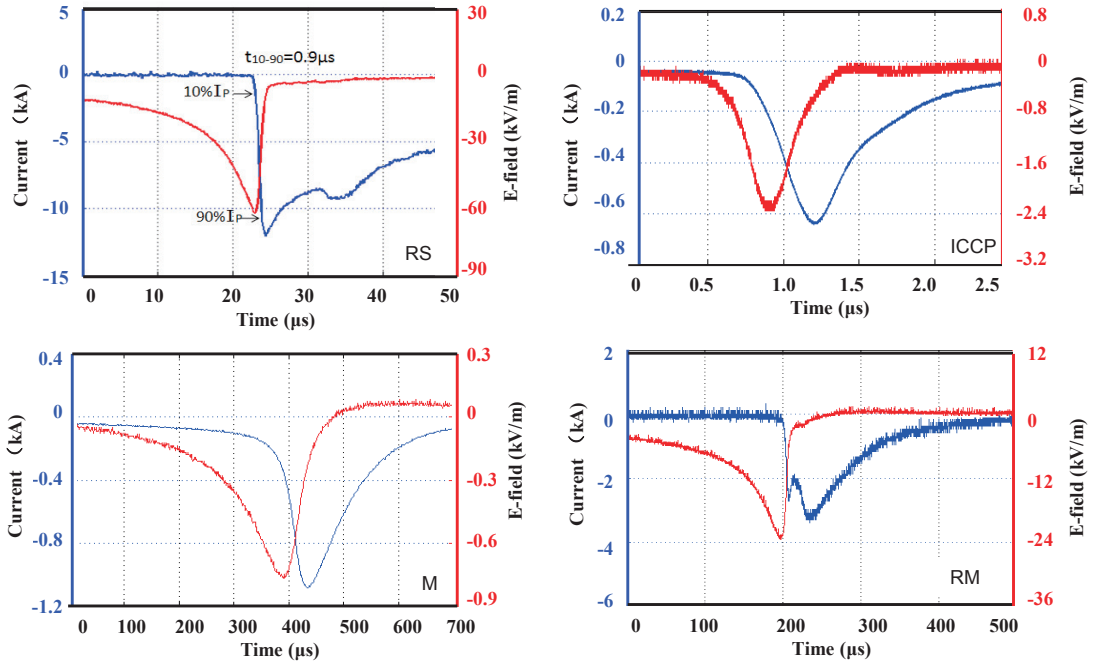

Fig. 6. Waveform example of current and close electric field at 60 m from the discharge channel for the RS, M-event, ICCP and RM event documented in Zhanhua, Shandong.

Table 1 compares the RS parameters of rocket-triggered lightning from the two sites. The GM values of the peak current, half peak width, risetime from 10% to 90% peak, and charge transfer for the RSs were found to be 12.1 kA, 14.8 μs, 1.0 μs and 0.86 C, respectively, while they were 0.28 kA, 242 μs, 251 μs and 0.10 C for the M-components, and 0.09 kA, 712 μs, 437 μs and 0.10 C for the ICC pulses in SHATLE (Qie et al., 2014a). Some of the M-components might exhibit a peak current with several kilo-amperes (Jiang et al., 2011), comparable to some of the weak RSs. The charge transferred to the ground by an individual lightning discharge ranged from 6.3 C to 68.1 C.

Table 1. Main parameters of rocket-triggered negative lightning containing RSs in two sites.

Parameters	Zhanhua, Shandong (Qie et al., 2014a; Jiang et al., 2013a)				Conghua, Guangdong (Zheng et al., 2017)			
	N	AM	GM	Range	N	AM	GM	Range
Negative Flash								
Q_F (C)	12	33.3	26.9	6.3–68.1				
Multiplicity	12	4.5	3.3	1–16	48	4.6	3.3	1–13
Initial stage								
Duration	12	324.9	293.2	130.0–677.8	45	399.5	347.9	39.1–800.6
Average current (A)	12	81.9	67.5	48.5–140.6	45	153.3	132.5	55.0–685.3
Q_{IS} (C)	12	24.4	17.2	6.3–45.0	45	57.3	45.1	7.2–179.0
Individual Stroke								
Peak current (kA)	75	13.7	12.0	1.96–45.7	142	18.8	17.2	3.9–46.0
Risetime (μs)	75	1.7	0.7	0.09–18.8	142	0.5	0.4	0.2–7.8
Half peak width (μs)	75	24.0	14.1	1.0–112.0	142	21.6	17.9	4.7–67.0
Duration (ms)	75	6.3	3.3	1.0–59.0	142	41.4	13.4	0.6–591.9
Q_{RS} (C)	75	1.1	0.83	0.05–4.6	142	1.7	1.3	0.2–6.8

Notes: Rise time is from 10% to 90% of peak current; Q_{RS}, charge transfer integral within 1 ms for RS; stroke duration includes the RS and any following CC; t_{HPW}, half-peak width; Rise time rise time of between 10% and 90%.

Zheng et al. (2017) presented the current characteristics of the IS and RS of triggered negative lightning in GCOELD. The IS had GMs of 347.9 ms for duration, a 132.5 A average current, 45.1 C charge transfer and 10.0×10^3 A^2 s action integral, with larger values than those reported elsewhere. The RS featured a greater peak current, charge transfer and action integral within 1 ms, but a shorter 10% to 90% rise time than elsewhere. A triggered lightning flash containing RSs tended to last longer and neutralize fewer charges during its IS than that without RSs. The RSs seem stronger in Conghua than in Zhanhua in view of the peak current and charge transfer.

Zheng et al. (2013) investigated the currents of IS RSs (ISRSs) in two altitude-triggered lightning flashes with gaps of 17 m and 50 m from the wire lower end to the ground, and the peak current was 10.19 kA and 9.03 kA, respectively. They concluded that the current waves of ISRSs were similar to those of typical RSs in classical triggered flashes in terms of multiple parameters, except for the smaller charge transfer, half-peak width, and action integral of ISRSs.

Zhang et al. (2016d) found that M-components with small amplitude (< 0.5 kA) were necessary for a long CC, and named the phenomenon the "restricted zone". Some M-events with current exceeding 1 kA might result from fast positive streamers with a speed of about 10^7 m s^{-1}, or by a dart leader from other branches of the lightning channel while the channel of the CC is still existing (Zhang et al., 2018c). Zhou et al. (2013) calculated the correlation between current and luminosity of the lightning channel during the period of the ICC process and CC process following RSs, and the same variation trend between the channel CC current and the luminosity was found.

Jiang et al. (2013b) modified the M-components model based on Rakov's "two-wave" theory and confirmed that the M-component evolution through the lightning CC channel involved a downward process transferring negative charge to the lower channel from the upper part, and an upward process that neutralized the charge deposited by the downward process. Wang et al. (2012b) simulated the subsidiary peak in the current waveform of triggered lightning strokes, and four possibilities of subsidiary peaks were suggested: channel branching, the corona current, and flashover along the triggering wire in a previous unsuccessful launch, or reflection of the current.

4. Physical processes in natural lightning and attachment to the ground

Observation of lightning flashes has been conducted in several regions with different climatic or orographic features in China, including the Tibetan Plateau (Cao et al., 2011b; Wang et al., 2011b), Daxing'Anling (Wang et al., 2011a; Lu et al., 2013; Wu et al., 2013a), Beijing (Wu et al., 2016c, d; Li et al., 2017a), Qinghai (Li et al., 2012; Qu et al., 2012a, b; Zhang et al., 2015a), Guangdong (Lan et al., 2011; Zhang et al., 2016d) and the Yangtze–Huaihe river basin (Zhu et al., 2014, 2015). Some of the main results are outlined in the following subsections.

4.1. *Lightning initiation and preliminary breakdown process inside thunderstorms*

The preliminary breakdown process (PBP) and initial radiation pulses in CG lightning have been studied in terms of initiation height and pulse characteristics (Cao et al., 2011a; Zhang et al., 2013b, 2015c; Wang et al., 2014a; Wu et al., 2016a). Wu et al. (2016a) divided the PBP into an initial PBP and a subsequent PBP. They found that when multiple pulse clusters were included in the initial PBPs, the initial streamer exhibited a discontinuous channel with a stepped-manner propagation traveling downward or upward. Each step corresponded to a pulse cluster. Wang et al. (2016d), using the BLNet 3D location results, found a clear branched 3D structure of the PBP in a negative CG (-CG) flash. The PBP started at an altitude of about 6 km and developed downward

to about 3 km with a speed of 5.9×10^5 m s^{-1}. An intercloud (IC) discharge initiated from about 7.2 km and propagated upward to 10 km with a velocity of 4.8×10^5 m s^{-1}.

Three types of initial breakdown pulse trains in positive CG (+CG) lightning were recognized by Zhang et al. (2013b). The category of the pulse trains is the same in Beijing and Guangzhou, but with different percentages of each category. Zhang et al. (2015c) analyzed the characteristics of bipolar pulse trains involved in E-field waveforms of lightning discharges. They indicated that the ratio of the largest peak of the PB pulse train to that of the first RS was obviously larger in Beijing, perhaps because of the different scales of the lower positive charge region (LPCR) in thunderstorms in Beijing and Guangzhou.

4.2. *Downward negative leaders and chaotic pulse trains in -CG flashes*

Jiang et al. (2017) found that branching in downward negative leaders resulted from the multiple connections of clustered space leaders with the same parent channel, and connections occurred successively or almost simultaneously as some of the space leaders resurrected after their termination. The GM value of the step length was 4.4 m. The distance from the space leader center to the main channel tip was about 3.6 m. More than 50% of steps occurred within ±30° from the direction of the advancing leader. Qi et al. (2016) detected a total of 23 space stems/leaders from a natural downward negative lightning discharge about 350 m away. The mean 2D length was 5 m, varying from 1 to 13 m. The mean distance between the bright segments and the main leader channel tip was about 4 m, ranging from 1 to 8 m.

Lan et al. (2011) reported direct measurements of the broadband EM field radiated from chaotic pulse trains (CPTs) associated with the leader-subsequent strokes in -CG lightning, and found that the corresponding channel extension speed was 2×10^7 m s^{-1}. Zhang et al. (2016c) found that 44% of subsequent strokes were preceded by CPTs and almost all CPTs were characterized by strong luminosity. Qiu et al. (2015) found that the chaotic leader propagated at a speed of (1.0–2.9) $\times10^7$ m s^{-1} and the duration of the CPT was 300–700 μs. The chaotic fluctuations were believed to be related to the continuous VHF radiation.

4.3. *Physical processes of high structure initiated lightning*

High spatial and temporal resolution lightning data have enabled many details involved in upward lightning from high structures in China to be revealed (Lu et al., 2012, 2013, 2015, 2016b; Gao et al., 2014; Jiang et al., 2014a, 2014b, 2014c; Qi et al., 2016; Zhang et al., 2017a; Wang et al., 2016e; 2018c).

Lu et al. (2013) found a negative lightning discharge exhibiting unexpected attachment behaviour with the tip of the downward leader connecting to the lateral surface of an upward connecting leader (UCL). The connecting behaviour of the upward leaders and the downward leader involved in the attachment process preceding the first RS could be divided into three types: a downward leader tip to the UCL tip, a downward leader tip to the UCL lateral surface, and a hybrid type that is a combination of the above two. The three types accounted for 42%, 50% and 8% of all the events, respectively. Lu et al. (2012) found that the unconnecting upward leader (UUL), initiated by the downward leader before a new striking point, propagated 1 km from the inception point. The 3D length for the six UCLs ranged from 180 m to 818 m, while the 3D speed ranged from 0.8×10^5 m s^{-1} to 14.3×10^5 m s^{-1} (Gao et al., 2014). The average 3D speed can be 1.3 times larger than the corresponding 2D speed. The 3D speed for both the UCL and UUL exhibited a trend of increasing after their inception, while the downward leader did not show a clear variation trend (Lu et al., 2015).

Jiang et al. (2014b) and Yuan et al. (2017) conducted observations of lightning flashes striking at a 325 m high tower. They found that 95% of the 20 cases were initiated from the tower, and most of them were induced by nearby +CG flashes. The approach of in-cloud horizontal negative leader during the +CG is a vital condition for the inception of the upward leader from the tower. The other-triggered lightning-was more likely to occur in the thunderstorm dissipation stage, with a relatively lower cloud top and weaker radar echo, whereas self-initiating lightning tended to occur in the mature stage of the thundercloud and the stratiform region of the thundercloud trailed by the convective line was above the tower.

Wang et al. (2016e) presented a detailed picture of the stepping process in a UPL initiated from the 325 m high tower. It was found that the stepping process of the UPL occurred as an abrupt extension of the leader channel accompanied by a burst of corona streamer from the fresh leader top. The burst of corona streamer at the end of the stepping process was significantly brighter than the enhancing streamer zone when the stepping process started. The mean value of the step length was 4.9 m, and the interstep interval was 62 μs. The average speed of the leader propagation was 8.1×10^4 m s^{-1}, while the mean speed of channel extension for an individual step should be higher than 7.3×10^5 m s^{-1}, which is almost an order of magnitude larger than the average leader propagation speed. Jiang et al. (2014a) documented the bidirectional leader propagation through a pre-existing channel created by a UPL from a high structure, similar to the bidirectional leader in the rocket-triggered lightning mentioned above (Qie et al., 2017).

The existence of high structures affects the lightning activity around them. Zhang et al. (2017a) found that the flash or stroke density showed a considerable increase around the Canton Tower within a radius of 1 km and a clear radial decrease from 1 km to 4 km. The LLS-inferred stroke peak current occurred around the Canton Tower showed an obvious increase within a radius of 1 km.

4.4. *Attachment processes and ground terminations in -CG flashes*

Substantial progress has been made in the past few years in understanding the processes of lightning attachment. The

attachment process and associated leader behavior for natural lightning were captured by high-speed camera and VHF interferometer measurements. For stepped leader-first RSs, Jiang et al. (2015) found that the UCLs were more likely to be initiated by those brighter downward branches with lower tips, and there was a greater possibility that they might achieve attachment. The UCLs in two leader-subsequent stroke processes exhibited relatively long lengths, at 340 m and 105 m for the two cases, respectively. Evidence concerning the mechanism for multiple groundings has been provided by sensitive broadband VHF interferometers. It was revealed that multiple-ground terminations of a negative lightning event resulted from either the multiple termination strokes or forked stroke with the same main leader channel, or from the different branches of the PBP inside the cloud (Sun et al., 2016).

4.5. *Positive and bipolar CG lightning flashes*

Although just around 10% of all natural CG lightning flashes are of positive polarity, they tend to be more intense and possess greater potential damage than negative flashes. Qie et al. (2013) investigated +CG lightning characteristics in the Daxing'Anling forest region. They documented 185 +CG flashes containing 196 RSs and showed that 71.9% of all +CG discharges contained a CC process, and 94.6% of all the +CG flashes were single-stroke flashes. About 15.1% of the +CG flashes were a kind of byproduct of IC flashes.

Kong et al. (2015) found that the speed of five positive downward leaders increased as they approached the ground, with an average 2D speed ranging from 0.3×10^5 m s^{-1} to 2.0×10^5 m s^{-1}. Approximately 67.4% of the 89 observed +CG flashes accompanied a prior long-lasting intense IC discharge ranging from about 100 ms to 973 ms, suggesting that a previous in-cloud discharge is conducive to +CG flashes.

Chen et al. (2015) observed a downward bipolar lightning discharge hit at a 90 m tall object. The six negative strokes developed along the same discharge channel with the first positive RS. The velocity of the RS ranged from 1.0 to 1.3×10^8 m s^{-1}. The leader before the positive RS developed downward with a 2D velocity of 2.5×10^6 m s^{-1} without obvious branches. Tian et al. (2016) found that the onset of the bipolar flash was followed by extension of several positive leaders near the cloud bottom, and one of them developed downward culminating with a positive stroke with a long CC. Another positive leader propagated horizontally toward a possible far negative charge center and initiated several recoil leaders that sporadically retrograded in the discharge channel. Finally, three recoil leaders developed along the positive stroke path and induced negative strokes respectively, which ultimately resulted in the polarity reversal of the following RSs.

4.6. *Propagation of lightning-radiated EM field*

The lightning-radiated EM signal propagates along the ground surface, and its far EM field is an important parameter for accurately locating lightning. The effects of lightning EM field propagation along a ground surface path with different characteristics (Zhang et al., 2012a, c), and a rough surface (Zhang et al., 2012b; Li et al., 2014), have been widely studied. Zhang et al. (2015b) studied the propagation effect of frequency-dependent soil on the far vertical E-fields radiated by subsequent lightning strikes to tall objects. They found that the field propagation attenuation along frequency-dependent soil is obviously less than the case where the parameters are assumed to be constant. Hou et al. (2018a, b) presented a new approximating method for lightning-radiated extremely low frequency (ELF) and VLF ground wave propagation over intermediate ranges within 1500 km from lightning strike points, and it was found that the curvature of the earth had a much greater effect on the field propagation at intermediate ranges than the earth's finite conductivity, and the lightning-radiated ELF/VLF E-field peak value (V m^{-1}) at intermediate ranges yielded a propagation distance d (km) dependence of $d^{-1.32}$. The effect of a tall tower on the conversion factors from the EM field to the channel current has also been studied, by Zhang et al. (2014a, 2015b).

4.7. *Direct and indirect effects of lightning*

Triggered lightning has become an important technique in testing the direct and indirect effects of lightning. Zhang et al. (2013a) investigated the induced overvoltage on a vertical signal line of an aerovane from an automatic weather station when lightning was triggered nearby. Chen et al. (2016) analyzed the features of the residual voltage in the Surge Protective Devices (SPD) connected to an overhead distribution line and ground during triggered lightning. The residual voltage of the SPD linked to the overhead line was affected by the ground potential rise (GPR) at the SPD grounding point. The SPD residual voltage is usually determined by the induced voltage on the overhead distribution line by the RS and big M-component processes (Chen et al., 2018b). A long-duration induction current might come to the SPD from the ground because of the GPR effect. The SPD's residual voltage might last up to an order of milliseconds and damage the SPD. The average gradient of the triggering lightning current is a very important parameter in determining the peak current and surge energy through SPDs (Chen et al., 2018a). Liu et al. (2015) proposed a tangential E-field technique based on the EM field to estimate the critical E-field of soil ionization, which is significant for the performance of a grounding system of lightning protection. The instant moment of the soil ionization can be found by checking the tangential component of the horizontal E-field.

5. Lightning activities and charge structure in thunderstorms

Ground-based lightning location data and space-based lightning data have been widely used to study statistically the characteristics of lightning in different regions (Wu et al., 2013b, 2016b; Xia et al., 2015; Li et al., 2016; Zheng et al., 2016a), or lightning activities in different kinds of thunderstorms in China (Wu et al., 2013a; Xie et al., 2015; Zhang et al., 2017c).

5.1. *Lightning climatology in different regions*

Based on spaced-based Lightning Imaging Sensor and Optical Transient Detector (LIS/OTD) data, Zhu et al. (2013) found that the global flash density was 46.2 fl s^{-1} and nearly 78.1% of them occurred in the region of 30°S–30°N. The ratio of lightning density over land to that over the ocean was 9.6:1. Variation in lightning density with altitude was represented by two peaks and three valleys, with the former appearing at 100–2400 m and 3300–4600 m, and the latter appearing below 100 m, at 2400–3300 m, and above 4600 m. Zheng et al. (2016a, b) found that CG flashes over land showed only one peak in the afternoon, while those over offshore waters showed peaks in the morning and afternoon. The diurnal variations of small-current CG lightning (peak current $\leqslant$ 50 kA) and large-current CG lightning (peak current > 50 kA, > 75 kA and > 100 kA) were much more different over the ocean, but similar over the continent.

The Northwest Pacific region is affected by diversified climatic systems and exhibits unique weather patterns. Zhang et al. (2018b) analyzed the climatology of lightning activity over the Northwest Pacific using WWLLN data for the period 2005–15. It was found that the maximum lightning densities were along the coast of Southeast Asia and the tropical islands. The strongest lightning activity appeared in the monsoon season in the central and southern South China Sea. Yuan et al. (2016) found that the lightning anomaly showed significant positive correlation with Oceanic Niño Index over both East China and Indonesia during El Niño episodes, while no obvious correlation was found during La Niña episodes. Significantly increased lightning activity was also found for larger convective available potential energy (CAPE).

The relationship between lightning and precipitation for short-duration rainfall events in the Beijing region was analyzed during the summer seasons from 2006 to 2007 by Wu et al. (2017, 2018). They developed a nowcasting method for short-duration rainfall (i.e., < 6 h) events in terms of rainfall and lightning jumps. It was found that the approach provided early warnings for the associated short-duration rainfall events from the regional scale to meso-γ scale. Xia et al. (2018) classified mesoscale convective systems (MCSs) into four categories based on their high/low convective rainfall rates (HR/LR) and high/low CG lightning frequencies (HL/LL). They found that the HRHL, HRLL, LRHL, and LRLL categories exhibited orders of the highest-to-smallest CAPE and perceptible water, but the smallest-to-largest convective inhibition and lifted indices.

5.2. *Lightning activity and charge structure in the plateau region*

Many unique features of lightning and charge structure in the Chinese Inland Plateau or Tibetan Plateau region have been discovered since the 1980s. Recently, in-situ E-field sounding and 3D lightning mapping results showed some promising new results on these issues.

Li et al. (2017b) analyzed the evolution of the charge structure inferred from 3D VHF lightning mapping data for a small thunderstorm in Qinghai region. During the initial developing stage and the mature stage of the thundercloud, the charge structure exhibited a steady negative dipole, i.e., a negative above a positive charge region. During the dissipation stage of the thundercloud, the charge structure changed to a more complicated one, resulting from the merger of two convective cells. A positive-charge dipole, negative-charge dipole, and tripole charge structure coexisted in different regions of the thunderstorm during its late stage. Fan et al. (2018b) found a positive tripole charge structure during most stages of a hailstorm with a larger LPCR in the thunderstorm, resulting in a low +CG rate. Wang et al. (2013) found some kind of interaction between nearby lightning discharges, i.e., the following lightning discharges would be suppressed by the lightning discharges before. However, the prior lightning discharge might provide a preconditioned channel to facilitate the following lightning discharges. Fan et al. (2014) developed an overlap and progressive method using either a one-point charge model or point dipole model, and found that the charge neutralized in the negative charge layer by the CC of lightning flashes usually ranged from 2.5 km to 4.7 km above the ground in Qinghai region.

By conducting balloon-borne E-field sounding in Pingliang, Gansu Province, Zhang et al. (2018a) found five charge centers in the cloud region colder than 0°C, and the polarity of charge regions alternated vertically, with the lowest region being positive. Two other charge layers were located near the cloud base, with the negative region below the positive. Zhang et al. (2012d) suggested that the LPCR intensity of thunderstorms in the Chinese Inland Plateau region was likely determined by the quantity of graupel, based on the vertical distribution of each type of precipitation particle inferred from data from an X-band dual linear polarization Doppler radar.

Figure 7 shows a schematic illustration of the charge structure evolution of a typical plateau thunderstorm based on previous studies. The outstanding characteristics of the plateau thunderstorm charge structure are the development of an inverted dipole (positive charge region below negative charge region) and the upper positive charge region may develop in the mature stage of the storm to form a tripole charge structure with a larger-than-usual lower positive charge region (refer to Figure 7a), or may not develop to form just an inverted dipole charge structure (refer to Figure 7b). In both cases, the inverted polarity IC flashes are observed frequently in the Chinese Inland and Tibetan plateau regions. In the later stage or the dissipating stage, the charge structure of the thunderstorm could be a normal dipole or normal tripole, with descent of the positively charged graupel particles from the lower part of the thundercloud.

5.3. *Lightning characteristics and charge structure in convective systems*

Several cases of squall line systems have been analyzed based on SAFIR3000 or BLNet whole lightning data in the Beijing area (Liu et al., 2011, 2013a, b; Xu et al., 2016c; Sun

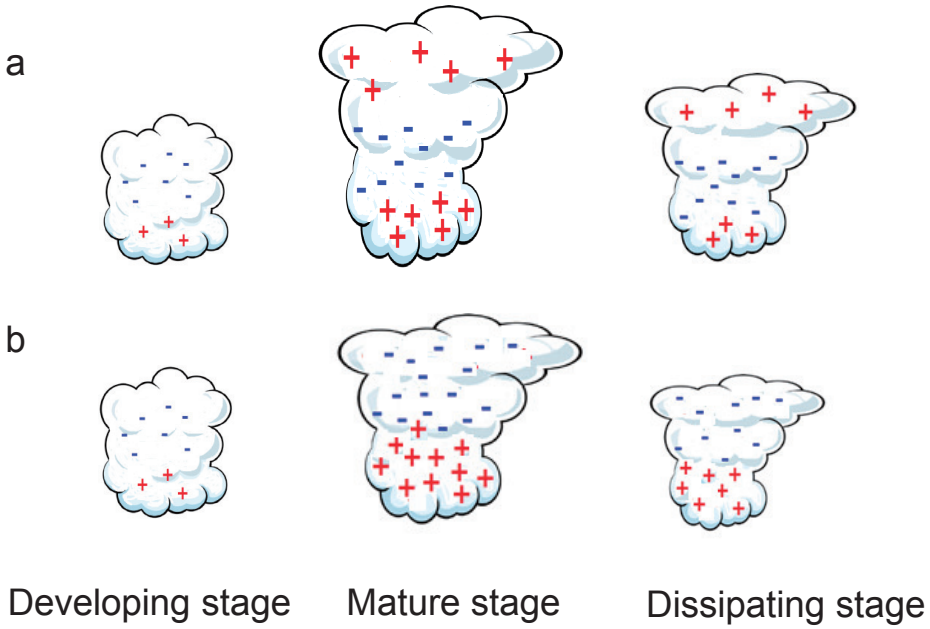

Fig. 7. Schematic illustrations of the charge structure evolution of a typical plateau thunderstorm.

et al., 2018a; Xu et al., 2018). Liu et al. (2013b) found that most of the lightning radiation sources were located horizontally in the squall line with higher radar reflectivity. The distribution of radiation sources developed vertically from two layers into three layers. In the developing stage of the convective system, the upper-layer center of the radiation sources was located at about 11 km, while the lower layer centered at about 4 km. In the mature stage of the convective system, the entire convective line was characterized by a multilayer charge structure with three positive charge layers located at 5 km, 9.5 km, and 13 km, and two negative charge layers at 7 km and 11 km, respectively. Xu et al. (2018) discussed the lightning activity in squall lines with a cell merging process, and found that lightning peaked after the cell merging in most of the studied cases. About 85% of lightning flashes were distributed within the 10 km range of the convection line, while quite a few were in the stratiform region. The majority of lightning was concentrated in the region with strong vertical wind shear (VWS), and the positive CG (PCG) was more likely to occur in the transition zone and stratiform region. Wang et al. (2016b) found that the dominant polarity of the stratiform CG flashes was different from that of the CG flashes in the convective region. The current of the first RS of the stratiform CG flashes was usually greater than that of the convective CG flashes. The location of the stratiform CG flashes was always near or at the edge of a region with the bright band, but never directly below the reflectivity core in the bright band.

Wang et al. (2017a) found that the grounding location of nearly 79.1% of CG flashes was underneath the cloud region with vertical velocity at the 0°C layer ranging from −5 m s^{-1} to 5 m s^{-1}, and the majority of the locations were under the weak updraft region. The bright band showed a close relationship with the lightning initiation near the 0°C isotherm in the stratiform region (Wang et al., 2018a).

Some hailstorms have been found to contain two stages with high-rate lightning activity divided by a low lightning rate (Zheng et al., 2009; Xu et al., 2016c). The first peak is usually before the hailfall and the second peak after the hailfall, with the greater peak in the second stage. In two hailstorms, the dominant polarity of CG lightning around the first lightning peak was positive and changed to negative around the second lightning peak. The change in polarity resulted from the evolution of the charge structure from an inverted one during the first stage to a normal one during the second stage.

Supporting by 3D lightning location data with the capability of describing the channel structure of flashes, Zhang et al. (2017e) reported that the mean flash size was inversely correlated to the flash rate, with a correlation coefficient of −0.87 following a unary power function. It was more likely that thunderstorms with relatively weak convection and high precipitation corresponded to CG lightning with a large peak current. The charge pockets and horizontally broad charge regions were employed to explain the relationships of flash density with flash size or intensity (Zheng et al., 2016b).

5.4. *Narrow bipolar events and indication of lightning initiation*

Narrow bipolar events (NBEs), sometimes referred as compact intracloud discharges (CIDs), are a distinct type of intercloud lightning flashes characterized by a narrow bipolar EM pulse with a timescale of 10 μs to 20 μs, and produce powerful VHF radiation.

Liu et al. (2012) mapped the discharge channel images of CIDs by using VHF interferometers and indicated that the CIDs tended to develop vertically with a scale ranging from 0.40 km to 1.9 km and an average velocity from 0.44×10^8 m

s^{-1} to 1.0×10^{8} m s^{-1}. Wang et al. (2012d) found 32 out of 236 CIDs in isolation, while 204 of them were accompanied by either IC or CG flashes. Among the latter, a total of 130 were more likely to trigger lightning, while 72 were in the middle of lightning discharges, and the other two terminated lightning. The peak power of the CIDs always occurred between an altitude of 7 km and 16 km, and ranged from 12 kW to 781 kW in the frequency band from 267 MHz to 273 MHz.

Wu et al. (2011) found that the ratio of -CIDs appears to increase with the intensity of the convection. Zhang et al. (2016a) developed a 3D locating method for NBEs based on a two-axis magnetic sensor and ionospheric reflection pairs. They found that NBEs were mainly produced in the convective region with an echo intensity $\geqslant$ 30 dBZ. Positive NBEs were predominately produced between 7 km and 15 km, while -NBEs were above 14 km. The NBEs that occurred in Northeast China were observed to be consistent with the results of those in other regions (Lü et al., 2013a, b)

5.5. *Lightning activity in Typhoons over the Northwest Pacific*

Tropical cyclones (TCs) are a major weather process in the Northwest Pacific. Pan et al. (2010) found a peak value of lightning flashes in the eyewall region, a minimum in the inner rain band, and a strong maximum in the outer rain band for seven super typhoons over the Northwest Pacific. This bimodal pattern of lightning distribution has been verified by recent research (Pan et al., 2013, 2014; Wang et al., 2016a, 2017b, 2018b). Zhang et al. (2015d) analyzed the lightning activities in 116 TCs in the years from 2005 to 2009 in the Northwest Pacific using WWLLN lightning data. They indicated that weak storms (tropical depressions and tropical storms) were more likely to produce lightning than very strong storms (typhoons and super typhoons). TCs that strengthened in the next 24 h exhibited higher lightning density than those that weakened. The lightning density inside the inner core was larger for rapid intensification cases than for rapid weakening cases, suggesting a predictive effect of inner-core lightning on TC rapid intensity change. Pan et al. (2014) found that the correlation coefficient between the total flashes within a radius of 600 km and the maximum wind speed for weak and super typhoons from 2005 to 2009 was 0.81 and 0.74, respectively. For about 78% of the super typhoons, the peak lightning rate was prior to the maximum wind speed, and the most common lead time was about 30 h, while it was 60 h for 56% of weak typhoons, indicating that the lightning rate could be used as a measure of typhoon intensification.

Wang et al. (2018b) found that the variation in flash rate with sea surface temperature showed a positive correlation for 280 TCs from 2005 to 2016 over the Northwest Pacific. The VWS dominated the downshear left (right) asymmetric lightning distribution of the inner core (outer rain bands), and this asymmetry became more significant as the wind shear increased. The asymmetry of lightning distribution in the inner core was related to the joint effects of the VWS and TC motion vectors; however, the asymmetry in the outer rainband was more closely related to the VWS. The inner core asymmetry weakened when the TC was moving fast in the direction that was opposite or to the right of the VWS.

5.6. *Numerical simulation of lightning and electrification inside thunderstorms*

Numerical simulation of lightning and electrification inside thunderstorms has been conducted in several groups (Tan et al., 2012, 2014c, 2016; Wang et al., 2016c; Guo et al., 2017). Liu et al. (2014) adopted the noninductive electrification mechanism, i.e., the Takahashi78 scheme and Saunders98 scheme, and lightning parameterization into the RAMSV6.0 model. The simulation showed that the thunderstorm exhibited a tripole charge structure with the Takahashi78 scheme, while the charge structure changed from dipole to tripole with the Saunders98 scheme. The simulated lightning rate was in good agreement with the observation.

Xu et al. (2012, 2014) and Zhao et al. (2015) introduced electrification schemes into the WRF model, and developed WRF-Electric models. The numerical experiments on the charge structure evolution of a hailstorm suggested that the inverted charge structure could be produced through a so-called dynamical-derived mechanism (Xu et al., 2016a). Simulation of Typhoon Molave (2009) showed that the charge structure in the eyewall exhibited a positive tripole prior to its landfall by using WRF-Electric (Xu et al., 2016b). It became a negative dipole with negative charge in the middle and positive charge below after Molave reached its maximum intensity. The charge structure in the eyewall was closely related to the typhoon intensity, but not directly correlated to the landfall. The convective cells in the outer rain band exhibited a positive tripole or positive dipole charge structure in different stages of Typhoon Molave.

Wang et al. (2015a, b) found that ice particles with vertical velocity ranging from 1 m s^{-1} to 5 m s^{-1} accumulated the most charge during all stages of a thunderstorm. An updraft with speeds between -1 m s^{-1} and 1 m s^{-1} was the most favorable for charge separation. The vertical velocity at the initiation locations of lightning flashes was correlated to the maximum updraft speed with a cubic polynomial. The graupel mixing ratios at the initiation sites correlated linearly with the mixing ratios of the graupel concentration center. This linear correlation was significant in the active and the later stage of the thunderstorm (Wang et al., 2017c).

Aerosol effects on thunderstorm electrification and lightning frequency have been studied using numerical simulation (Shi et al., 2015; Zhao et al., 2015). Zhao et al. (2015) found that increased aerosol loading resulted in a large increasing rate of snow and graupel, as well as a larger ice particle density, and the electrification process in the thunderstorm enhanced consequently.

Tan et al. (2014a) studied impacts of the LPCR on lightning type using a lightning-resolving model. They found that the LPCR was crucial in producing -CG and inverted -IC flashes. Increasing the LPCR charge density or extension, lightning changed from +IC-dominated to -CG lightning–dominated, and then to inverted IC flashes–dominated. The

charge density of the LPCR played a major role in the determination of lightning type compared with extension of the LPCR. It was only when the LPCR maximum charge density was within a certain range that -CG flashes occurred, and the probability of -CG flashes was almost constant. The potential at the lightning initiation point was a crucial parameter to determine whether the leader propagated to the ground (Tan et al., 2014b). The initiation potential for CG lightning was > 30 MV, while that for IC lightning was typically < 30 MV. Because the space charge determines the environmental potential, the lightning type also depends on the relative position and magnitude of charge regions near the lightning initiation position. Sun et al. (2018b) discussed the feedback effect of E-field force on electrification and charge structure in thunderstorms based on the NSSL WRF-Electric model; the overall influences of the E-field force on electrification tended to be positive, and its feedback effect on the thunderstorm structure should not be neglected.

5.7. *Lightning data assimilation in cloud-resolving numerical models*

Lightning data assimilation methods have been investigated and tested in cloud-resolving numerical models to improve the forecasting of convection and precipitation. Qie et al. (2014b) constructed an empirical formula between lightning rate and the mixing ratio of the cloud ice particle, including graupel, ice and snow. The established functions were nudged into the WRF model. The intensity and location of the strong convection were significantly improved 1 h after the lightning assimilation. The precipitation center, amount and coverage were improved too, and they were all much closer to the observation than that without lightning assimilation. Chen et al. (2017) developed a new lightning data assimilation scheme with comprehensive nudging of water content. Both the low-level water vapor and graupel mass in the mixing phase region were nudged according to the detected total lightning flash rate and model conditions. The bulk Richardson number was adopted to measure the dynamic and thermodynamic conditions and as an index to nudge the lightning. The simulation showed that the new scheme better matched the observation in terms of convection and precipitation. Zhang et al. (2017b) assimilated lightning data using the 3D variational data assimilation method in the WRF-3DVar system in cycling mode with an interval of 10 min based on empirical functions between lightning frequency and the mixing ratio of water vapor. The results for a squall line system indicated that 60 min was the appropriate time-window for lightning assimilation. Forecasting of accumulated precipitation in 1 h during the assimilation and the accumulated precipitation in the following 3 h were greatly improved.

Wang et al. (2014b) used the CG lightning rate to adjust the vertical velocity, specific humidity and specific cloud water content in a model using a physical initialization method, based on a relationship between lightning flash density and reflectivity. The forecasted convection was improved with the lightning-proxy reflectivity assimilation scheme. The reflectivity prediction was significantly improved and maintained for about 3 h.

Wang et al. (2018c) developed a lightning assimilation scheme based on time-lagged ensembles. With the assimilation method, the background error covariance was calculated using time-lagged ensembles. The graupel mixing ratio was retrieved from the observed lightning rate by using empirical vertical profiles (Wang et al., 2017d). The observation errors were estimated by using uncertainties in lightning data and the retrieved vertical profiles. Assimilating lightning data for a severe convective event exhibited many observed convective cells that did not appear in the control run; plus, it restrained the appearance of false convection and decreased the shifting errors of convection.

Li et al. (2016) simulated the occurrence of lightning by using a modified lightning potential index and observed lightning data. The lightning density was calculated by differentiating the ice mass of precipitation and non-precipitation. The proposed method was examined for a quasi-linear MCS using the WRF model and 3D variation analysis system in the ARPS model. The simulation suggested that most lightning flashes occurred on the right side and at the front of the MCSs, where the surface wind field converged intensely. The lightning flashes tended to occur in the regions with a large gradient of CAPE.

6. Effects of thunderstorms on the upper atmosphere

The middle and upper atmosphere including lower ionosphere is dynamically perturbed by the underlying thunderstorms. Observations on transient luminous events (TLEs), including sprites, elves, blue jets, blue starters, halos and gigantic jets (GJs) occurring above thunderstorms have been continuously conducted since 2007. The relationship of TLEs with the parent lightning and thunderstorm has been the main subject in the last few years. In addition, effects of the thunderstorms on the ionosphere have also been investigated.

6.1. *TLEs and their parent lightning and thunderstorm*

Yang and Feng (2012) reported a GJ produced by a multicell thunderstorm in the coast region (Yellow Sea) in eastern China. The relationship between the GJ occurrence time and the strong convection has been confirmed. However, based on data analysis, Yang et al. (2018a) also found that the GJ was produced during summer thunderstorms in the midlatitude region without strong updrafts, as indicated by the maximum echo top along the GJ azimuth being lower than the regional tropopause. Different from other summer thunderstorms just producing GJs during their evolutions, two sprites were also observed in a time window containing the GJ in the study of Yang et al. (2018a), suggesting that the meteorological characteristics of the GJ-producing storms has not yet been fully understood. By using data from the lightning imager onboard the FORMOSAT-2 satellite and a ground-based lightning location network, Liu et al. (2018a) suggested that the negative NBEs were probably the initial part of the blue jets, as ev-

idenced by the fact that the negative NBEs were concurrent with six of the seven blue jets by less than 1 ms.

Sprites are the most easily observed TLEs in ground-based observation. A sprit-producing thunderstorm usually produces several or even many sprites. However, compared with thunderstorms that may induce hundreds of TLEs in the High Plain region in the United States, thunderstorms in China are usually observed to produce several or tens of sprites (Yang et al., 2013a, b; Wang et al., 2015d; Huang et al., 2018), and some storms even produce just a single sprite during its life cycle (Yang et al., 2017a). No significant differences in the particle (i.e., precipitation ice, cloud ice and cloud water content) distributions have been found among many-, one- and non-sprite-producing storms. Most sprites are caused by positive strokes (Yang et al., 2013a, b) and the following CC (Yang et al., 2015, 2017a), but they can also be initiated by -CG flashes (Yang et al., 2017b). Compared with many positive sprites, negative sprite events are rare. Yang et al. (2018b) reported five sprites over an MCS, and one of them was confirmed to be negative by both the local LLS and ELF magnetic field, and another was only confirmed to be negative by the local LLS data. They also found that sprites with different polarity were located in distinct regions of the MCS; the negative sprites were associated with strong convection and large wind shear, and positive ones were above the stratiform region. Negative sprite events could be produced by lightning strokes with a not very large peak current.

6.2. *Thunderstorm effects on the ionosphere*

The ionosphere's characteristics can be affected by underlying thunderstorms. Yu et al. (2015) found that enhancement of the ionospheric sporadic E-layer likely resulted from powerful lightning strokes. Yu et al. (2017) showed a significant increase in the neutral metal Na layer above thunderstorms, and the thunderstorm-associated gravity waves and E-field could be possible reasons. Xu et al. (2015) studied two concentric gravity wave events launched by underlying thunderstorms. They showed that the horizontal waves of the first event propagated freely within 300 km from the thunderstorm center, but the second event was induced by two strong thunderstorms exhibiting multiscale waves with different horizontal wavelengths.

High-energy particles related to thunderstorms are also a very interesting topic. Wang et al. (2012c) found that the E-field of thunderstorm could affect the counting rate of the Neutron Monitor at Yangbajing over Tibetan Plateau region. Because of absorption in the atmosphere, ground-based measurement of high-energy particles is difficult; coordinated ground- and space-based observations and theoretical work are needed to further investigate this issue.

7. Summary and outstanding scientific questions

Although substantial progress has been made in recent years in understanding lightning discharge processes and their effects, a number of mysteries still remain. As described above, new detection technology holds promise for future advancements in our understanding of lightning and its relationships with other subjects. The following is a summary of some of the outstanding scientific questions that remain to be addressed:

The first and perhaps most interesting question concerns the detailed nature of lightning initiation and its relationship with terrestrial gamma-ray flashes (TGFs), as well as energetic in-cloud pulses (EIPs) with ultra-high currents > 200 kA. It is becoming evident that TGFs are likely to be produced during initial breakdown processes, and EIPs could be a highly energetic form of initial breakdown pulses. The relationship between TGFs and lightning initiation and the detailed processes that produce TGFs are still the largest mystery and should be paid more attention in China.

The second outstanding question concerns the nature of fast breakdown associated with high-power NBEs, which also seems to be responsible for initiating lightning. VHF mapping interferometer and 3D VHF location joint observations with continuously improving capability will play a critical role in revealing more features of fast breakdown and answering how fast breakdown is produced.

The third question concerns how kinematic and microphysical properties of storms affect electrification and lightning. In particular, how does ice microphysics affect electrification processes? Polarimetric radars, in-situ particle and E-field sensors, together with improving broadband interferometers and 3D lightning mapping systems hold promise for addressing these outstanding questions. The FY-4 Geosynchronous Lightning Mapping Imager will allow us for the first time to study lightning continuously in geographic regions that have been inaccessible to ground-based lightning location networks. It is expected to allow us to make considerable progress in our understanding of lightning in oceanic thunderstorms, in TCs and in mountainous thunderstorms.

In conclusion, figuring out the various facets of the mysteries of lightning is obviously a primary subject of interest, and needs to be continuously studied by the atmospheric electricity community.

Acknowledgements. The research was supported by the National Natural Science Foundation of China (Grant No. 41630425) and the National Key Basic Research Program of China (Grant No. 2014CB441401).

REFERENCES

Cao, D. J., X. S. Qie, J. Yang, J. F. Wang, and D. F. Wang, 2011a: Analysis on characteristics of sub-microsecond electric field change waveform during the initial stage of lightning discharge. *Chinese Journal of Atmospheric Sciences*, **35**(4), 645–656, https://doi.org/10.3878/j.issn.1006-9895.2011.04.05. (in Chinese with English abstract)

Cao, D. J., L. Y. Tian, J. Xiao, J. Yang, J. F. Wang, and D. F. Wang, 2011b: A fast recording, display and waveform analysis system on multi-parameter of lightning flash. *Plateau Meteorol-*

ogy, **30**(2), 518–524. (in Chinese with English abstract)

Cao, D. J., X. S. Qie, S. Duan, Y. J. Xuan, and D. F. Wang, 2012: Lightning discharge process based on short-baseline lightning VHF radiation source locating system. *Acta Physica Sinica*, **61**(6), 069202, https://doi.org/10.7498/aps.61.069202. (in Chinese with English abstract)

Chen, L. W., Y. J. Zhang, W. T. Lu, D. Zheng, Y. Zhang, S. D. Chen, and Z. H. Huang, 2012: Performance evaluation for a lightning location system based on observations of artificially triggered lightning and natural lightning flashes. *J. Atmos. Oceanic Technol.*, **29**, 1835–1844, https://doi.org/10.1175/JTECH-D-12-00028.1.

Chen, L. W., W. T. Lu, Y. J. Zhang, and D. H. Wang, 2015: Optical progression characteristics of an interesting natural downward bipolar lightning flash. *J. Geophys. Res.*, **120**, 708–715, https://doi.org/10.1002/2014JD022463.

Chen, S. D., Y. J. Zhang, C. Chen, X. Yan, W. T. Lu, and Y. Zhang, 2016: Influence of the ground potential rise on the residual voltage of low-voltage surge protective devices due to nearby lightning flashes. *IEEE Transactions on Power Delivery*, **31**(2), 596–604, https://doi.org/10.1109/TPWRD.2015.2441773.

Chen, S. D., Y. J. Zhang, M. Zhou, X. Yan, W. T. Lu, and Y. Zhang, 2018a: Influence on low-voltage surge protective devices of overhead distribution lines due to nearby return strokes. *IEEE Transactions on Power Delivery*, **33**, 1099–1106, https://doi.org/10.1109/TPWRD.2017.2695662.

Chen, S. D., Y. J. Zhang, M. Zhou, X. Yan, W. T. Lu, L. W. Chen, and Y. Zhang, 2018b: Observation of residual voltage in low-voltage surge protective devices due to nearby m-components. *IEEE Transactions on Electromagnetic Compatibility*, **60**(3), 776–784, https://doi.org/10.1109/TEMC.2017.2737648.

Chen, Z. X., X. S. Qie, Y. Tian, D. F. Wang, and S. F. Yuan, 2017: Assimilation of lightning data through comprehensively nudging water contents at the cloud-resolving scale. *Acta Meteorologica Sinica*, **75**(3), 442–459, https://doi.org/10.11676/qxxb2017.035. (in Chinese with English abstract)

Dong, W. S., X. S. Liu, Y. J. Zhang, and G. S. Zhang, 2002: Observations on the leader-return stroke of cloud-to-ground lightning with the broadband interferometer. *Science in China Series D*: *Earth Sciences*, **45**, 259–269, https://doi.org/10.1360/02yd9028.

Fan, P. L., D. Zheng, Y. J. Zhang, S. Q. Gu, W. J. Zhang, W. Yao, B. W. Yan, and Y. B. Xu, 2018a: A performance evaluation of the World Wide Lightning Location Network (WWLLN) over the Tibetan Plateau. *J. Atmos. Oceanic Technol.*, **35**, 927–939, https://doi.org/10.1175/JTECH-D-17-0144.1.

Fan, X. P., G. S. Zhang, Y. H. Wang, Y. J. Li, T. Zhang, and B. Wu, 2014: Analyzing the transmission structures of long continuing current processes from negative ground flashes on the Qinghai-Tibetan Plateau. *J. Geophys. Res.*, **119**, 2050–2063, https://doi.org/10.1002/2013JD020402.

Fan, X. P., Y. J. Zhang, G. S. Zhang, and D. Zheng, 2018b: Lightning characteristics and electric charge structure of a hail-producing thunderstorm on the eastern Qinghai-Tibetan plateau. *Atmosphere*, **9**, 295, https://doi.org/10.3390/atmos9080295.

Fan, X. P., Y. J. Zhang, D. Zheng, Y. Zhang, W. T. Lu, H. Y. Liu, and L. T. Xu, 2018c: A new method of three-dimensional location for low-frequency electric field detection array. *J. Geophys. Res.*, **123**, 8792–8812, https://doi.org/10.1029/2017JD028249.

Fan, Y. F., G. P. Lu, R. B. Jiang, H. B. Zhang, M. Y. Liu, and X. S. Qie, 2017: Application of low-frequency magnetic sensor for remote measurement of the initial continuous current in rocket-triggering lightning. *Chinese Journal of Atmospheric Sciences*, **41**(5), 1027–1036, https://doi.org/10.3878/j.issn.1006-9895.1702.16248. (in Chinese with English abstract)

Fan, Y. F., and Coauthors, 2018d: Characteristics of electromagnetic signals during the initial stage of negative rocket-triggered lightning. *J. Geophys. Res.*, **123**, 11 625–11 636, https://doi.org/10.1029/2018JD028744.

Gao, Y., W. T. Lu, Y. Ma, L. W. Chen, Y. Zhang, X. Yan, and Y. J. Zhang, 2014: Three-dimensional propagation characteristics of the upward connecting leaders in six negative tall-object flashes in Guangzhou. *Atmospheric Research*, **149**, 193–203, https://doi.org/10.1016/j.atmosres.2014.06.008.

Guo, F. X., Y. Li, Z. C. Huang, M. F. Wang, F. H. Zeng, C. H. Lian, and Y. J. Mu, 2017: Numerical simulation of 23 June 2016 Yancheng City EF4 tornadic supercell and analysis of lightning activity. *Science China Earth Sciences*, **60**(12), 2204–2213, https://doi.org/10.1007/s11430-017-9109-8.

Hou, W. H., Q. L. Zhang, L. Wang, and J. B. Zhang, 2018a: Effect of striking a cone-shaped mountain top on the far lightning-radiated electromagnetic field. *IEEE Transactions on Electromagnetic Compatibility*, https://doi.org/10.1109/TEMC.2018.2843772. (in press)

Hou, W. H., Q. L. Zhang, J. B. Zhang, L. Wang, and Y. Shen, 2018b: A new approximate method for lightning-radiated ELF/VLF ground wave propagation over intermediate ranges. *International Journal of Antennas and Propagation*, Article ID 9353294, https://doi.org/10.1155/2018/9353294.

Huang, A. J., G. P. Lu, H. B. Zhang, F. F. Liu, B. Y. Zhu, J. Yang, and Z. C. Wang, 2018: Locating parent lightning strokes of sprites observed over a mesoscale convective system in Shandong Province, China. *Adv. Atmos. Sci.*, **35**(11), 1396–1414, https://doi.org/10.1007/s00376-018-7306-4.

Jiang, R., X. Qie, J. Yang, C. Wang, and Y. Zhao, 2013b: Characteristics of M-component in rocket-triggered lightning and a discussion on its mechanism. *Radio Sci.*, **48**, 597–606, https://doi.org/10.1002/rds.20065.

Jiang, R. B., and Coauthors, 2011: Lightning *M*-components with peak currents of kilo amperes and their mechanism. *Acta Physica Sinica*, **60**(7), 079201. (in Chinese with English abstract)

Jiang, R. B., X. S. Qie, C. X. Wang, and J. Yang, 2013a: Propagating features of upward positive leaders in the initial stage of rocket-triggered lightning. *Atmospheric Research*, **129–130**, 90–96, https://doi.org/10.1016/j.atmosres.2012.09.005.

Jiang, R. B., Z. J. Wu, X. S. Qie, D. F. Wang, and M. Y. Liu, 2014a: High-speed video evidence of a dart leader with bidirectional development. *Geophys. Res. Lett.*, **41**, 5246–5250, https://doi.org/10.1002/2014GL060585.

Jiang, R. B., X. S. Qie, Z. J. Wu, D. F. Wang, M. Y. Liu, G. P. Lu, and D. X. Liu, 2014b: Characteristics of upward lightning from a 325-m-tall meteorology tower. *Atmospheric Research*, **149**, 111–119, https://doi.org/10.1016/j.atmosres.2014.06.007.

Jiang, R. B., Z. L. Sun, and Z. J. Wu, 2014c: Concurrent upward lightning flashes from two towers. *Atmospheric and Oceanic Science Letters*, **7**(3), 260–264, https://doi.org/10.3878/j.issn.1674-2834.13.0099.

Jiang, R. B., X. S. Qie, Z. C. Wang, H. B. Zhang, G. P. Lu, Z. L.

Sun, M. Y. Liu, and X. Li, 2015: Characteristics of lightning leader propagation and ground attachment. *J. Geophys. Res.*, **120**, 11 988-12 002, https://doi.org/10.1002/2015JD023519.

Jiang, R. B., X. S. Qie, H. B. Zhang, M. Y. Liu, Z. L. Sun, G. P. Lu, Z. C. Wang, and Y. Wang, 2017: Channel branching and zigzagging in negative cloud-to-ground lightning. *Scientific Reports*, **7**, 3457, https://doi.org/10.1038/s41598-017-03686-w.

Kong, X. Z., Y. Zhao, T. Zhang, and H. B. Wang, 2015: Optical and electrical characteristics of in-cloud discharge activity and downward leaders in positive cloud-to-ground lightning flashes. *Atmospheric Research*, **160**, 28–38, https://doi.org/10.1016/j.atmosres.2015.02.014.

Lan, Y., Y. J. Zhang, W. S. Dong, W. T. Lu, H. Y. Liu, and D. Zheng, 2011: Broadband analysis of chaotic pulse trains generated by negative cloud-to-ground lightning discharge. *J. Geophys. Res.*, **116**, D17109, https://doi.org/10.1029/2010JD015159.

Li, D. S., Q. L. Zhang, Z. H. Wang, and T. Liu, 2014: Computation of lightning horizontal field over the two-dimensional rough ground by using the three-dimensional FDTD. *IEEE Transactions on Electromagnetic Compatibility*, **56**(1), 143–148, https://doi.org/10.1109/TEMC.2013.2266479.

Li, X., X. S. Qie, K. Liu, Y. Wang, D. F. Wang, M. Y. Liu, Z. L. Sun, and H. B. Zhang, 2017a: Characteristics of cloud-to-ground lightning return strokes in Beijing based on high temporal resolution data of fast electric field change. *Climatic and Environmental Research*, **22**(2), 231–241, https://doi.org/10.3878/j.issn.1006-9585.2016.16007. (in Chinese with English abstract)

Li, W. L., X. S. Qie, S. M. Fu, D. B. Su, and Y. H. Shen, 2016: Simulation of quasi-linear mesoscale convective systems in northern China: Lightning activities and storm structure. *Adv. Atmos. Sci.*, **33**(1), 85–100, https://doi.org/10.1007/s00376-015-4170-3.

Li, Y. J., G. S. Zhang, J. Wen, Y. H. Wang, T. Zhang, X. P. Fan, and B. Wu, 2012: Spatial and temporal evolution of a multicell thunderstorm charge structure in coastal areas. *Chinese Journal of Geophysics*, **55**(10), 3203–3212. (in Chinese with English abstract)

Li, Y. J., G. S. Zhang, J. Wen, D. H. Wang, Y. H. Wang, T. Zhang, X. P. Fan, and B. Wu, 2013: Electrical structure of a Qinghai-Tibet Plateau thunderstorm based on three-dimensional lightning mapping. *Atmospheric Research*, **134**, 137–149, https://doi.org/10.1016/j.atmosres.2013.07.020.

Li, Y. J., G. S. Zhang, Y. H. Wang, B. Wu, and J. Li, 2017b: Observation and analysis of electrical structure change and diversity in thunderstorms on the Qinghai-Tibet Plateau. *Atmospheric Research*, **194**, 130–141, https://doi.org/10.1016/j.atmosres.2017.04.031.

Liu, D. X., X. S. Qie, Y. J. Xiong, and G. L. Feng, 2011: Evolution of the total lightning activity in a leading-line and trailing stratiform mesoscale convective system over Beijing. *Adv. Atmos. Sci.*, **28**(4), 866–878, https://doi.org/10.1007/s00376-010-0001-8.

Liu, D. X., X. S. Qie, L. X. Pan, and L. Peng, 2013a: Some characteristics of lightning activity and radiation source distribution in a squall line over north China. *Atmospheric Research*, **132–133**, 423–433, https://doi.org/10.1016/j.atmosres.2013.06.010.

Liu, D. X., X. S. Qie, Z. C. Wang, X. K. Wu, and L. X. Pan, 2013b: Characteristics of lightning radiation source distribution and charge structure of squall line. *Acta Physica Sinica*, **62**(21), 219201, https://doi.org/10.7498/aps.62.219201. (in Chinese with English abstract)

Liu, D. X., X. S. Qie, L. Peng, and W. L. Li, 2014: Charge structure of a summer thunderstorm in North China: Simulation using a regional atmospheric model system. *Adv. Atmos. Sci.*, **31**, 1022–1034, https://doi.org/10.1007/s00376-014-3078-7.

Liu, F. F., and Coauthors, 2018a: Observations of blue discharges associated with negative narrow bipolar events in active deep convection. *Geophys. Res. Lett.*, **45**, 2842–2851, https://doi.org/10.1002/2017GL076207.

Liu, H. Y., W. S. Dong, T. Wu, D. Zheng, and Y. J. Zhang, 2012: Observation of compact intracloud discharges using VHF broadband interferometers. *J. Geophys. Res.*, **117**, D01203, https://doi.org/10.1029/2011JD016185.

Liu, H. Y., S. Qiu, and W. S. Dong, 2018b: The three-dimensional locating of VHF broadband lightning interferometers. *Atmosphere*, **9**, 317, https://doi.org/10.3390/atmos9080317.

Liu, K., X. S. Qie, J. X. He, G. P. Lu, and Q. Xia, 2015: Estimation of critical electric field of soil ionisation based on tangential electric field method. *IET Science, Measurement & Technology*, **9**(6), 758–764, https://doi.org/10.1049/iet-smt.2014.0352.

Lu, G. P., R. B. Jiang, X. S. Qie, H. B. Zhang, Z. L. Sun, M. Y. Liu, Z. C. Wang, and K. Liu, 2014: Burst of intracloud current pulses during the initial continuous current in a rocket-triggered lightning flash. *Geophys. Res. Lett.*, **41**, 9174–9181, https://doi.org/10.1002/2014GL062127.

Lu, G. P., and Coauthors, 2016a: Characterization of initial current pulses in negative rocket-triggered lightning with sensitive magnetic sensor. *Radio Sci.*, **51**, 1432–1444, https://doi.org/10.1002/2016RS005945.

Lu, G. P., and Coauthors, 2018: Measurement of continuing charge transfer in rocket-triggered lightning with low-frequency magnetic sensor at close range. *Journal of Atmospheric and Solar-Terrestrial Physics*, **175**, 76–86, https://doi.org/10.1016/j.jastp.2018.02.010.

Lu, W. T., and Coauthors, 2012: Characteristics of unconnected upward leaders initiated from tall structures observed in Guangzhou. *J. Geophys. Res.*, **117**, D19211, https://doi.org/10.1029/2012JD018035.

Lu, W. T., L. W. Chen, Y. Ma, V. A. Rakov, Y. Gao, Y. Zhang, Q. Y. Yin, and Y. J. Zhang, 2013: Lightning attachment process involving connection of the downward negative leader to the lateral surface of the upward connecting leader. *Geophys. Res. Lett.*, **40**, 5531–5535, https://doi.org/10.1002/2013GL058060.

Lu, W. T., and Coauthors, 2015: Three-dimensional propagation characteristics of the leaders in the attachment process of a downward negative lightning flash. *Journal of Atmospheric and Solar-Terrestrial Physics*, **136**, 23–30, https://doi.org/10.1016/j.jastp.2015.07.011.

Lu, W. T., Q. Qi, Y. Ma, L. W. Chen, X. Yan, V. A. Rakov, D. H. Wang, and Y. J. Zhang, 2016b: Two basic leader connection scenarios observed in negative lightning attachment process. *High Voltage*, **1**(1), 11–17, https://doi.org/10.1049/hve.2016.0002.

Lü, F. C., B. Y. Zhu, H. L. Zhou, V. A. Rakov, W. W. Xu, and Z. L. Qin, 2013a: Observations of compact intracloud lightning discharges in the northernmost region (51°N) of China. *J. Geophys. Res.*, **118**, 4458–4465, https://doi.org/10.1002/jgrd.50295.

Lü, F. C., B. Y. Zhu, M. Ma, L. X. Wei, and D. Ma, 2013b: Observations of narrow bipolar events during two thunderstorms in Northeast China. *Science China Earth Sciences*, **56**(8), 1459–1470, https://doi.org/10.1007/s11430-012-4484-2.

Pan, L. X., X. S. Qie, D. X. Liu, D. F. Wang, and J. Yang, 2010: The lightning activities in super typhoons over the Northwest Pacific. *Science China Earth Sciences*, **53**, 1241–1248, https://doi.org/10.1007/s11430-010-3034-z.

Pan, L. X., D. X. Liu, X. S. Qie, D. F. Wang, and R. P. Zhu, 2013: Land-sea contrast in the lightning diurnal variation as observed by the WWLLN and LIS/OTD data. *Acta Meteorologica Sinica*, **27**(4), 591–600, https://doi.org/10.1007/s13351-013-0408-0.

Pan, L. X., X. S. Qie, and D. F. Wang, 2014: Lightning activity and its relation to the intensity of typhoons over the Northwest Pacific Ocean. *Adv. Atmos. Sci.*, **31**(3), 581–592, https://doi.org/10.1007/s00376-013-3115-y.

Pu, Y. J., R. B. Jiang, X. S. Qie, M. Y. Liu, H. B. Zhang, Y. F. Fan, and X. K. Wu, 2017: Upward negative leaders in positive triggered lightning: Stepping and branching in the initial stage. *Geophys. Res. Lett.*, **44**, 7029–7035, https://doi.org/10.1002/2017GL074228.

Qi, Q., W. T. Lu, Y. Ma, L. W. Chen, Y. J. Zhang, and V. A. Rakov, 2016: High-speed video observations of the fine structure of a natural negative stepped leader at close distance. *Atmospheric Research*, **178–179**, 260–267, https://doi.org/10.1016/j.atmosres.2016.03.027.

Qie, X. S., 2012: Progresses in the atmospheric electricity researches in China during 2006-2010. *Adv. Atmos. Sci.*, **29**(5), 993–1005, https://doi.org/10.1007/s00376-011-1195-0.

Qie, X. S., R. B. Jiang, C. X. Wang, J. Yang, J. F. Wang, and D. X. Liu, 2011: Simultaneously measured current, luminosity, and electric field pulses in a rocket-triggered lightning flash. *J. Geophys. Res.*, **116**, D10102, https://doi.org/10.1029/2010JD015331.

Qie, X. S., J. Yang, R. B. Jiang, C. X. Wang, G. L. Feng, S. J. Wu, and G. S. Zhang, 2012: Shandong Artificially Triggering Lightning Experiment and current characterization of return stroke. *Chinese Journal of Atmospheric Sciences*, **36**(1), 77–88, https://doi.org/10.3878/j.issn.1006-9895.2012.01.07. (in Chinese with English abstract)

Qie, X. S., Z. C. Wang, D. F. Wang, and M. Y. Liu, 2013: Characteristics of positive cloud-to-ground lightning in Da Hinggan Ling forest region at relatively high latitude, northeastern China. *J. Geophys. Res.*, **118**, 13 393–13 404, https://doi.org/10.1002/2013JD020093.

Qie, X. S., R. B. Jiang, and J. Yang, 2014a: Characteristics of current pulses in rocket-triggered lightning. *Atmospheric Research*, **135–136**, 322–329, https://doi.org/10.1016/j.atmosres.2012.11.012.

Qie, X. S., R. P. Zhu, T. Yuan, X. K. Wu, W. L. Li, and D. X. Liu, 2014b: Application of total-lightning data assimilation in a mesoscale convective system based on the WRF model. *Atmospheric Research*, **145–146**, 255–266, https://doi.org/10.1016/j.atmosres.2014.04.012.

Qie, X. S., and Coauthors, 2017: Bi-directional leader development in a preexisting channel as observed in rocket-triggered lightning flashes. *J. Geophys. Res.*, **122**, 586–599, https://doi.org/10.1002/2016JD025224.

Qiu, S., Z. D. Jiang, L. H. Shi, Z. C. Niu, and P. Zhang, 2015: Characteristics of negative lightning leaders to ground observed by TVLS. *Journal of Atmospheric and Solar-Terrestrial Physics*, **136**, 31–38, https://doi.org/10.1016/j.jastp.2015.07.008.

Qu, H. Y., P. Yuan, H. M. Zhang, and X. S. Qie, 2012a: Evolution characteristic of near-infrared spectra and temperature along the stroke channel of lightning discharge process. *Chinese Journal of Geophysics*, **55**(8), 2508–2513, https://doi.org/10.6038/j.issn.0001-5733.2012.08.003. (in Chinese with English abstract)

Qu, H. Y., P. Yuan, T. L. Zhang, X. S. Qie, Y. J. Zhang, and G. S. Zhang, 2012b: Analysis on physical characteristic of lightning with multiple return strokes. *Plateau Meteorology*, **31**(1), 218–222. (in Chinese with English abstract)

Shi, D. D., D. Zheng, Y. Zhang, Y. J. Zhang, Z. G. Huang, W. T. Lu, S. D. Chen, and X. Yan, 2017: Low-frequency E-field Detection Array (LFEDA)—Construction and preliminary results. *Science China Earth Sciences*, **60**, 1896–1908, https://doi.org/10.1007/s11430-016-9093-9.

Shi, Z., Y. B. Tan, H. Q. Tang, J. Sun, Y. Yang, L. Peng, and X. F. Guo, 2015: Aerosol effect on the land-ocean contrast in thunderstorm electrification and lightning frequency. *Atmospheric Research*, **164–165**, 131–141, https://doi.org/10.1016/j.atmosres.2015.05.006.

Srivastava, A., and Coauthors, 2017: Performance assessment of Beijing Lightning Network (BLNET) and comparison with other lightning location networks across Beijing. *Atmospheric Research*, **197**, 76–83, https://doi.org/10.1016/j.atmosres.2017.06.026.

Sun, L., and Coauthors, 2018a: Evolution of lightning radiation sources of a strong squall line over Beijing metropolitan region and its relation to convection region and surface thermodynamic condition. *Chinese Journal of Atmospheric Sciences*, https://doi.org/10.3878/j.issn.1006-9895.1805.18128. (in press) (in Chinese with English abstract)

Sun, L., X. S. Qie, E. R. Mansell, Z. X. Chen, Y. Xu, R. B. Jiang, and Z. L. Sun, 2018b: Feedback effect of electric field force on electrification and charge structure in thunderstorm. *Acta Physica Sinica*, **67**(16), 169201. https://doi.org/10.7498/aps.67.20180505. (in Chinese with English abstract)

Sun, Z. L., X. S. Qie, M. Y. Liu, D. J. Cao, and D. F. Wang, 2013: Lightning VHF radiation location system based on short-baseline TDOA technique—Validation in rocket-triggered lightning. *Atmospheric Research*, **129–130**, 58–66, https://doi.org/10.1016/j.atmosres.2012.11.010.

Sun, Z. L., X. S. Qie, and M. Y. Liu, 2014a: Characteristics of a negative cloud-to-ground lightning discharge based on locations of VHF radiation sources. *Atmospheric and Oceanic Science Letters*, **7**(3), 248–253, https://doi.org/10.3878/j.issn.1674-2834.13.0110.

Sun, Z. L., X. S. Qie, R. B. Jiang, M. Y. Liu, X. K. Wu, Z. C. Wang, G. P. Lu, and H. B. Zhang, 2014b: Characteristics of a rocket-triggered lightning flash with large stroke number and the associated leader propagation. *J. Geophys. Res.*, **119**(23), 13 388–13 399, https://doi.org/10.1002/2014JD022100.

Sun, Z. L., X. S. Qie, and M. Y. Liu, 2015: Analysis on very high frequency radiation and development characteristics of a negative cloud-to-ground lightning discharge with multiple return strokes. *Chinese Journal of Atmospheric Sciences*, **39**(4), 667–676, https://doi.org/10.3878/j.issn.1006-9895.1410.14106. (in Chinese with English abstract)

Sun, Z. L., X. S. Qie, M. Y. Liu, R. B. Jiang, Z. C. Wang, and H. B. Zhang, 2016: Characteristics of a negative lightning with multiple-ground terminations observed by a VHF lightning location system. *J. Geophys. Res.*, **121**, 413–426, https://doi.

org/10.1002/2015JD023702.

Tan, Y., X. Guo, J. Zhu, Z. Shi, and D. Zhang, 2014c: Influence on simulation accuracy of atmospheric electric field around a building by space resolution. *Atmospheric Research*, **138**, 301–307, https://doi.org/10.1016/j.atmosres.2013.11.023.

Tian, Y., and Coauthors, 2016: Characteristics of a bipolar cloud-to-ground lightning flash containing a positive stroke followed by three negative strokes. *Atmospheric Research*, **176–177**, 222–230, https://doi.org/10.1016/j.atmosres.2016.02.023.

Tan, Y. B., Z. Shi, N. N. Wang, and X. F. Guo, 2012: Numerical simulation of the effects of randomness and characteristics of electrical environment on ground strike sites of cloud-to-ground lightning. *Chinese Journal of Geophysics*, **55**(11), 3534–3541. (in Chinese with English abstract)

Tan, Y. B., Z. W. Liang, Z. Shi, J. R. Zhu, and X. F. Guo, 2014a: Numerical simulation of the effect of lower positive charge region in thunderstorms on different types of lightning. *Science China Earth Sciences*, **57**, 2125–2134, https://doi.org/10.1007/s11430-014-4867-7.

Tan, Y. B., S. C. Tao, Z. W. Liang, and B. Y. Zhu, 2014b: Numerical study on relationship between lightning types and distribution of space charge and electric potential. *J. Geophys. Res.*, **119**, 1003–1014, https://doi.org/10.1002/2013JD019983.

Tan, Y. B., C. Chen, J. C. Zhou, B. W. Zhou, D. D. Zhang, and X. F. Guo, 2016: A parameterization scheme for upward lightning in the cloud model and a discussion of the initial favorable environmental characteristics in the cloud. *Science China Earth Sciences*, **59**(7), 1440–1453, https://doi.org/10.1007/s11430-016-5309-5.

Wang, C. X., R. B. Jiang, J. Yang, and M. Y. Liu, 2012a: Current subsidiary peak in triggered lightning strokes. *Radio Sci.*, **47**, RS4002, https://doi.org/10.1029/2011RS004933.

Wang, C. X., X. S. Qie, R. B. Jiang, and J. Yang, 2012b: Propagating properties of a upward positive leader in a negative triggered lightning. *Acta Physica Sinica*, **61**(3), 039203, https://doi.org/10.7498/aps.61.039203. (in Chinese with English abstract)

Wang, C. X., D. Zheng, Y. J. Zhang, and L. P. Liu, 2017a: Relationship between lightning activity and vertical airflow characteristics in thunderstorms. *Atmospheric Research*, **191**, 12–19, https://doi.org/10.1016/j.atmosres.2017.03.003.

Wang, C. X., Z. L. Sun, R. B. Jiang, Y. M. Tian, and X. S. Qie, 2018c: Characteristics of downward leaders in a cloud-to-ground lightning strike on a lightning rod. *Atmospheric Research*, **203**, 246–253, https://doi.org/10.1016/j.atmosres.2017.12.014.

Wang, D. F., and Coauthors, 2011a: Analyses on the characteristic of cloud-to-ground lightning flash in Da Hinggan ling forest region. *Chinese Journal of Atmospheric Sciences*, **35**(1), 147–156, https://doi.org/10.3878/j.issn.1006-9895.2011.01.12. (in Chinese with English abstract)

Wang, F., Y. J. Zhang, D. Zheng, and L. T. Xu, 2015a: Impact of the vertical velocity field on charging processes and charge separation in a simulated thunderstorm. *Journal of Meteorological Research*, **29**(2), 328–343, https://doi.org/10.1007/s13351-015-4023-0.

Wang, F., Y. J. Zhang, and D. Zheng, 2015b: Impact of updraft on neutralized charge rate by lightning in thunderstorms: A simulation case study. *Journal of Meteorological Research*, **29**(6), 997–1010, https://doi.org/10.1007/s13351-015-5023-9.

Wang, F., X. S. Qie, D. X. Liu, H. F. Shi, and A. Srivastava, 2016a: Lightning activity and its relationship with typhoon intensity and vertical wind shear for Super Typhoon Haiyan (1330). *Journal of Meteorological Research*, **30**(1), 117–127, https://doi.org/10.1007/s13351-016-4228-x.

Wang, F., Y. J. Zhang, H. Y. Liu, W. Yao, and Q. Meng, 2016b: Characteristics of cloud-to-ground lightning strikes in the stratiform regions of mesoscale convective systems. *Atmospheric Research*, **178–179**, 207–216, https://doi.org/10.1016/j.atmosres.2016.03.021.

Wang, F., X. S. Qie, and X. D. Cui, 2017b: Climatological characteristics of lightning activity within tropical cyclones and its relationship to cyclone intensity change over the Northwest Pacific. *Chinese Journal of Atmospheric Sciences*, **41**(6), 1167–1176, https://doi.org/10.3878/j.issn.1006-9895.1704.17102. (in Chinese with English abstract)

Wang, F., Y. J. Zhang, D. Zheng, L. T. Xu, W. J. Zhang, and Q. Meng, 2017c: Semi-idealized modeling of lightning initiation related to vertical air motion and cloud microphysics. *Journal of Meteorological Research*, **31**(5), 976–986, https://doi.org/10.1007/s13351-017-6201-8.

Wang, F., H. Y. Liu, W. S. Dong, Y. J. Zhang, and Q. Meng, 2018a: Characteristics of lightning flashes associated with the charge layer near the 0°C isotherm in the stratiform region of mesoscale onvective systems. *J. Geophys. Res.*, **123**, 9524–9541, https://doi.org/10.1029/2018JD028569.

Wang, F., X. S. Qie, D. F. Wang, and A. Srivastava, 2018b: Lightning activity in tropical cyclones and its relationship to dynamic and thermodynamic parameters over the northwest Pacific. *Atmospheric Research*, **213**, 86–96, https://doi.org/10.1016/j.atmosres.2018.05.027.

Wang, H. L., F. X. Guo, T. L. Zhao, M. O. Qin, and L. Zhang, 2016c: A numerical study of the positive cloud-to-ground flash from the forward flank of normal polarity thunderstorm. *Atmospheric Research*, **169**, 183–190, https://doi.org/10.1016/j.atmosres.2015.10.011.

Wang, H. L., and Coauthors, 2017d: Improving lightning and precipitation prediction of severe convection using lightning data assimilation with NCAR WRF-RTFDDA. *J. Geophys. Res.*, **122**, 12 296–12 316, https://doi.org/10.1002/2017JD027340.

Wang, H. L., and Coauthors, 2018d: Continuous assimilation of lightning data using time-lagged ensembles for a convection-allowing numerical weather prediction model. *J. Geophys. Res.*, **123**, 9652–9673, https://doi.org/10.1029/2018JD028494.

Wang, J. F., D. J. Cao, H. Lu, and D. F. Wang, 2011b: Characteristics of lightning activities in Yangbajing region of Tibet. *Plateau Meteorology*, **30**(3), 831–836. (in Chinese with English abstract)

Wang, J. F., X. S. Qie, H. Lu, J. L. Zhang, X. X. Yu, and F. Shi, 2012c: Effect of thunderstorm electric field on intensity of cosmic ray muons. *Acta Physica Sinica*, **61**(15), 159202, https://doi.org/10.7498/aps.61.159202. (in Chinese with English abstract)

Wang, Y., X. S. Qie, D. F. Wang, M. Y. Liu, and Z. C. Wang, 2014a: Comparisons of preliminary breakdown pulse trains in positive and negative cloud-to-ground lightning flashes. *Chinese Journal of Atmospheric Sciences*, **38**(1), 21–31, https://doi.org/10.3878/j.issn.1006-9895.2013.12167. (in Chinese with English abstract)

Wang, Y., Y. Yang, and C. H. Wang, 2014b: Improving forecasting of strong convection by assimilating cloud-to-ground

lightning data using the physical initialization method. *Atmospheric Research*, **150**, 31–41, https://doi.org/10.1016/j.atmosres.2014.06.017.

Wang, Y., and Coauthors, 2015c: Beijing Lightning NETwork (BLNET): Configuration and preliminary results of lightning location. *Chinese Journal of Atmospheric Sciences*, **39**(3), 571–582, https://doi.org/10.3878/j.issn.1006-9895.1407.14138. (in Chinese with English abstract)

Wang, Y., and Coauthors, 2016d: Beijing Lightning Network (BLNET) and the observation on preliminary breakdown processes. *Atmospheric Research*, **171**, 121–132, https://doi.org/10.1016/j.atmosres.2015.12.012.

Wang, Y. H., G. S. Zhang, X. S. Qie, D. H. Wang, T. Zhang, Y. X. Zhao, Y. J. Li, and T. L. Zhang, 2012d: Characteristics of compact intracloud discharges observed in a severe thunderstorm in northern part of China. *Journal of Atmospheric and Solar-Terrestrial Physics*, **84–85**, 7–14, https://doi.org/10.1016/j.jastp.2012.05.003.

Wang, Y. H., G. S. Zhang, T. Zhang, Y. J. Li, B. Wu, and T. L. Zhang, 2013: Interaction between adjacent lightning discharges in clouds. *Adv. Atmos. Sci.*, **30**(4), 1106–1116, https://doi.org/10.1007/s00376-012-2008-9.

Wang, Z. C., J. Yang, G. P. Lu, D. X. Liu, Y. Wang, X. Xiao, and X. S. Qie, 2015d: Sprites over a mesoscale convective system in north China and the corresponding characteristics of radar echo and lightning. *Chinese Journal of Atmospheric Sciences*, **39**(4), 839–848, https://doi.org/10.3878/j.issn.1006-9895.1412.14232. (in Chinese with English abstract)

Wang, Z. C., X. S. Qie, R. B. Jiang, C. X. Wang, G. P. Lu, Z. L. Sun, M. Y. Liu, and Y. J. Pu, 2016e: High-speed video observation of stepwise propagation of a natural upward positive leader. *J. Geophys. Res.*, **121**, 14 307–14 315, https://doi.org/10.1002/2016JD025605.

Wu, B., G. S. Zhang, J. Wen, T. Zhang, Y. J. Li, and Y. H. Wang, 2016a: Correlation analysis between initial preliminary breakdown process, the characteristic of radiation pulse, and the charge structure on the Qinghai-Tibetan Plateau. *J. Geophys. Res.*, **121**, 12 434–12 459, https://doi.org/10.1002/2016JD025281.

Wu, F., X. P. Cui, D. L. Zhang, D. X. Liu, and D. Zheng, 2016b. SAFIr-3000 lightning statistics over the Beijing metropolitan region during 2005-07. *Journal of Applied Meteorology and Climatology*, **55**, 2613–2633, https://doi.org/10.1175/JAMC-D-16-0030.1.

Wu, F., X. P. Cui, D. L. Zhang, and L. Qiao, 2017: The relationship of lightning activity and short-duration rainfall events during warm seasons over the Beijing metropolitan region. *Atmospheric Research*, **195**, 31–43, https://doi.org/10.1016/j.atmosres.2017.04.032.

Wu, F., X. P. Cui, and D. L. Zhang, 2018: A lightning-based nowcast-warning approach for short-duration rainfall events: Development and testing over Beijing during the warm seasons of 2006-2007. *Atmospheric Research*, **205**, 2–17, https://doi.org/10.1016/j.atmosres.2018.02.003.

Wu, T., W. S. Dong, Y. J. Zhang, and T. Wang, 2011: Comparison of positive and negative compact intracloud discharges. *J. Geophys. Res.*, **116**, D03111, https://doi.org/10.1029/2010JD015233.

Wu, X. K., T. Yuan, D. X. Liu, and G. L. Feng, 2013a: Study of the relationship between cloud-to-ground lightning and radar echo of a severe squall line in Shandong peninsula. *Plateau Meteorology*, **32**(2), 530–540. (in Chinese with English abstract)

Wu, Z. J., X. S. Qie, D. F. Wang, Y. J. Xuan, M. Y. Liu, and Z. C. Wang, 2013b: Retrieval of the charge sources neutralized by negative cloud-to-ground lightning flashes in the Daxing'anling Forest region. *Acta Meteorologica Sinica*, **71**(4), 783–796, https://doi.org/10.11676/qxxb2013.057. (in Chinese with English abstract)

Wu, Z. J., X. S. Qie, and D. F. Wang, 2016d: Characteristics of charge sources retrieved from the multi-station synchronous electric field change measurements of negative return-stroke. *Plateau Meteorology*, **35**(4), 1123–1134. (in Chinese with English abstract)

Wu, Z. J., X. S. Qie, D. F. Wang, and Y. Wang, 2016c: Charge transferred by the return stroke of negative cloud-to-ground lightning in the Beijing region. *Climatic and Environmental Research*, **21**(3), 247–257. (in Chinese with English abstract)

Xia, R. D., D. L. Zhang, and B. L. Wang, 2015: A 6-yr cloud-to-ground lightning climatology and its relationship to rainfall over central and Eastern China. *Journal of Applied Meteorology and Climatology*, **54**(12), 2443–2460, https://doi.org/10.1175/JAMC-D-15-0029.1.

Xia, R. D., D. L. Zhang, C. H. Zhang, and Y. Q. Wang, 2018: Synoptic control of convective rainfall rates and cloud-to-ground lightning frequencies in warm-season mesoscale convective systems over north China. *Mon. Wea. Rev.*, **146**(3), 813–831, https://doi.org/10.1175/MWR-D-17-0172.1.

Xie, Y. R., J. Wu, X. T. Liu, T. F. Zhang, Y. J. Xie, Y. J. Xu, and D. M. Zhao, 2015: Characteristics of cloud-to-ground lightning activity in hailstorms over Yunnan province. *Journal of Atmospheric and Solar-Terrestrial Physics*, **136**, 2–7, https://doi.org/10.1016/j.jastp.2015.10.011.

Xu, J. Y., and Coauthors, 2015: Concentric gravity waves over northern China observed by an airglow imager network and satellites. *J. Geophys. Res.*, **120**, 11 058–11 078, https://doi.org/10.1002/2015JD023786.

Xu, L. T., Y. J. Zhang, F. Wang, and D. Zheng, 2012: Coupling of electrification and discharge processes with WRF model and its preliminary verification. *Chinese Journal of Atmospheric Sciences*, **36**, 1041–1052, https://doi.org/10.3878/j.issn.1006-9895.2012.11235. (in Chinese with English abstract)

Xu, L. T., Y. J. Zhang, F. Wang, and D. Zheng, 2014: Simulation of the electrification of a tropical cyclone using the WRF-ARW model: An idealized case. *Journal of Meteorological Research*, **28**, 453–468, https://doi.org/10.1007/s13351-014-3079-6.

Xu, L. T., Y. J. Zhang, H. Y. Liu, D. Zheng, and F. Wang, 2016a: The role of dynamic transport in the formation of the inverted charge structure in a simulated hailstorm. *Science China Earth Sciences*, **59**, 1414–1426, https://doi.org/10.1007/s11430-016-5293-9.

Xu, L. T., Y. J. Zhang, W. J. Zhang, F. Wang, and D. Zheng, 2016b: Simulation of the evolution of the charge structure during the landfall of Typhoon Molave (2009). *Acta Meteorologica Sinica*, **74**, 1002–1016, https://doi.org/10.11676/qxxb2016.071. (in Chinese with English abstract)

Xu, S., D. Zheng, Y. Q. Wang, and P. Y. Hu, 2016c: Characteristics of the two active stages of lightning activity in two hailstorms. *Journal of Meteorological Research*, **30**(2), 265–281, https://doi.org/10.1007/s13351-016-5074-6.

Xu, Y., and Coauthors, 2018: Lightning activity of a severe squall line with cell merging process and its relationships with dynamic fields. *Chinese Journal of Atmospheric Sci-*

ences, **42**, 1393–1406, https://doi.org/10.3878/j.issn.1006-9895.1801.17220. (in Chinese with English abstract)

Yang, J., and G. L. Feng, 2012: A gigantic jet event observed over a thunderstorm in mainland China. *Chinese Science Bulletin*, **57**(36), 4791–4800, https://doi.org/10.1007/s11434-012-5486-3.

Yang, J., X. S. Qie, and G. L. Feng, 2013a: Characteristics of one sprite-producing summer thunderstorm. *Atmospheric Research*, **127**, 90–115, https://doi.org/10.1016/j.atmosres.2011.08.001.

Yang, J., M. R. Yang, C. Liu, and G. L. Feng, 2013b: Case studies of sprite-producing and non-sprite-producing summer thunderstorms. *Adv. Atmos. Sci.*, **30**(6), 1786–1808, https://doi.org/10.1007/s00376-013-2120-5.

Yang, J., G. P. Lu, L. J. Lee, and G. L. Feng, 2015: Long-delayed bright dancing sprite with large Horizontal displacement from its parent flash. *Journal of Atmospheric and Solar-Terrestrial Physics*, **129**, 1–5, https://doi.org/10.1016/j.jastp.2015.04.001.

Yang, J., G. P. Lu, N. Y. Liu, H. H. Cui, Y. Wang, and M. Cohen, 2017a: Analysis of a mesoscale convective system that produced a single sprite. *Adv. Atmos. Sci.*, **34**(2), 258–271, https://doi.org/10.1007/s00376-016-6092-0.

Yang, J., G. P. Lu, N. Y. Liu, M. Sato, G. L. Feng, Y. Wang, and J. K. Chou, 2017b: Sprite possibly produced by two distinct positive cloud-to-ground lightning flashes. *Terrestrial, Atmospheric and Oceanic Sciences*, **28**, 609–624, https://doi.org/10.3319/TAO.2016.07.22.01.

Yang, J., M. Sato, N. Y. Liu, G. P. Lu, Y. Wang, and Z. C. Wang, 2018a: A gigantic jet observed over an mesoscale convective system in midlatitude region. *J. Geophys. Res.*, **123**, 977–996, https://doi.org/10.1002/2017JD026878.

Yang, J., N. Y. Liu, M. Sato, G. P. Lu, Y. Wang, and G. L. Feng, 2018b: Characteristics of thunderstorm structure and lightning activity causing negative and positive sprites. *J. Geophys. Res.*, **123**, 8190–8207, https://doi.org/10.1029/2017JD026759.

Yu, B. K., and Coauthors, 2015: Evidence for lightning-associated enhancement of the ionospheric sporadic *E* layer dependent on lightning stroke energy. *J. Geophys. Res.*, **120**(10), 9202–9212, https://doi.org/10.1002/2015JA021575.

Yu, B. K., and Coauthors, 2017: The enhancement of neutral metal Na layer above thunderstorms. *Geophys. Res. Lett.*, **44**, 9555–9563, https://doi.org/10.1002/2017GL074977.

Yuan, S. F., R. B. Jiang, X. S. Qie, D. F. Wang, Z. L. Sun, and M. Y. Liu, 2017: Characteristics of upward lightning on the Beijing 325 m meteorology tower and corresponding thunderstorm conditions. *J. Geophys. Res.*, **122**, 12 093–12 105, https://doi.org/10.1002/2017JD027198.

Yuan, T., Y. L. Di, and K. Qie, 2016: Variability of lightning flash and thunderstorm over East/Southeast Asia on the ENSO time scales. *Atmospheric Research*, **169**, 377–390, https://doi.org/10.1016/j.atmosres.2015.10.022.

Zhang, C. X., W. T. Lu, L. W. Chen, Q. Qi, Y. Ma, W. Yao, and Y. J. Zhang, 2017a: Influence of the Canton Tower on the cloud-to-ground lightning in its vicinity. *J. Geophys. Res.*, **122**, 5943–5954, https://doi.org/10.1002/2016JD026229.

Zhang, G. S., Y. H. Wang, X. S. Qie, T. Zhang, Y. X. Zhao, Y. J. Li, and D. J. Cao, 2010: Using lightning locating system based on time-of-arrival technique to study three-dimensional lightning discharge processes. *Science China Earth Sciences*, **53**(4), 591–602, https://doi.org/10.1007/s11430-009-0116-x.

Zhang, G. S., Y. J. Li, Y. H. Wang, T. Zhang, B. Wu, and Y. X. Liu, 2015a: Experimental study on location accuracy of a 3D VHF lightning-radiation-source locating network. *Science China Earth Sciences*, **58**, 2034–2048, https://doi.org/10.1007/s11430-015-5119-1.

Zhang, H. B., and Coauthors, 2016a: Locating narrow bipolar events with single-station measurement of low-frequency magnetic fields. *Journal of Atmospheric and Solar-Terrestrial Physics*, **143–144**, 88–101, https://doi.org/10.1016/j.jastp.2016.03.009.

Zhang, Q., L. X. He, T. T. Ji, and W. H. Hou, 2014a: On the field-to-current conversion factors for lightning strike to tall objects considering the finitely conducting ground. *J. Geophys. Res.*, **119**, 8189–8200, https://doi.org/10.1002/2014JD021496.

Zhang, Q. L., J. Yang, X. Q. Jing, D. S. Li, and Z. H. Wang, 2012a: Propagation effect of a fractal rough ground boundary on the lightning-radiated vertical electric field. *Atmospheric Research*, **104–105**, 202–208, https://doi.org/10.1016/j.atmosres.2011.10.009.

Zhang, Q. L., J. Yang, D. S. Li, and Z. H. Wang, 2012b: Propagation effects of a fractal rough ocean surface on the vertical electric field generated by lightning return strokes. *Journal of Electrostatics*, **70**(1), 54–59, https://doi.org/10.1016/j.elstat.2011.10.003.

Zhang, Q. L., M. Y. Liu, J. Yang, X. D. Liu, J. Yang, and R. B. Jiang, 2012c: Characteristics of the close leader/return stroke electric field change and its response to the corresponding charge density along the lightning channel. *Acta Meteorologica Sinica*, **70**(4), 847–854, https://doi.org/10.11676/qxxb2012.070. (in Chinese with English abstract)

Zhang, Q. L., W. H. Hou, T. T. Ji, L. X. He, and J. F. Su, 2014b: Validation and revision of far-field-current relationship for the lightning strike to electrically short objects. *Journal of Atmospheric and Solar-Terrestrial Physics*, **120**, 41–50, https://doi.org/10.1016/j.jastp.2014.08.015.

Zhang, Q. L., T. T. Ji, and W. H. Hou, 2015b: Effect of frequency-dependent soil on the propagation of electromagnetic fields radiated by subsequent lightning strike to tall objects. *IEEE Transactions on Electromagnetic Compatibility*, **57**(1), 112–120, https://doi.org/10.1109/TEMC.2014.2361926.

Zhang, R., Y. J. Zhang, L. T. Xu, D. Zheng, and W. Yao, 2017b: Assimilation of total lightning data using the three-dimensional variational method at convection-allowing resolution. *Journal of Meteorological Research*, **31**, 731–746, https://doi.org/10.1007/s13351-017-6133-3.

Zhang, T. L., J. Yang, R. Z. Chu, G. Zhao, and T. Zhang, 2012d: Distribution of precipitation particle and electrical characteristic of a thunderstorm in Pingliang region. *Plateau Meteorology*, **31**(4), 1091–1099. (in Chinese with English abstract)

Zhang, T. L., G. Zhao, C. X. Wei, Y. Gao, H. Yu, and F. C. Zhou, 2017c: Relationships between cloud-to-ground flashes and hydrometeors in a thunderstorm in Fujian province. *Journal of Atmospheric and Solar-Terrestrial Physics*, **154**, 226–235, https://doi.org/10.1016/j.jastp.2015.11.007.

Zhang, T. L., H. Yu, F. C. Zhou, J. Chen, and M. H. Zhang, 2018a: Measurements of vertical electric field in a thunderstorm in a Chinese inland plateau. *Annales Geophysicae*, **36**(4), 979–986, https://doi.org/10.5194/angeo-36-979-2018.

Zhang, W. J., Y. J. Zhang, D. Zheng, F. Wang, and L. T. Xu, 2015d: Relationship between lightning activity and tropical cyclone intensity over the northwest Pacific. *J. Geophys. Res.*, **120**, 4072–4089, https://doi.org/10.1002/2014JD022334.

Zhang, W. J., Y. J. Zhang, D. Zheng, L. T. Xu, and W. T. Lyu, 2018b: Lightning climatology over the northwest Pacific region: An 11-year study using data from the World Wide Lightning Location Network. *Atmospheric Research*, **210**, 41–57, https://doi.org/10.1016/j.atmosres.2018.04.013.

Zhang, Y., Y. J. Zhang, W. T. Lu, and D. Zheng, 2013b: Analysis and comparison of initial breakdown pulses for positive cloud-to-ground flashes observed in Beijing and Guangzhou. *Atmospheric Research*, **129–130**, 34–41, https://doi.org/10.1016/j.atmosres.2013.03.006.

Zhang, Y., Y. J. Zhang, D. Zheng, and W. T. Lu, 2015c: Preliminary breakdown, following lightning discharge processes and lower positive charge region. *Atmospheric Research*, **161–162**, 52–56, https://doi.org/10.1016/j.atmosres.2015.03.017.

Zhang, Y., Y. J. Zhang, C. Li, W. T. Lu, and D. Zheng, 2016c: Simultaneous optical and electrical observations of "chaotic" leaders preceding subsequent return strokes. *Atmospheric Research*, **170**, 131–139, https://doi.org/10.1016/j.atmosres.2015.11.012.

Zhang, Y., Y. J. Zhang, M. Xie, D. Zheng, W. T. Lu, S. D. Chen, and X. Yan, 2016d: Characteristics and correlation of return stroke, M component and continuing current for triggered lightning. *Electric Power Systems Research*, **139**, 10–15, https://doi.org/10.1016/j.epsr.2015.11.024.

Zhang, Y., P. R. Krehbiel, Y. J. Zhang, W. T. Lu, D. Zheng, L. T. Xu, and Z. G. Huang, 2017d: Observations of the initial stage of a rocket-and-wire-triggered lightning discharge. *Geophys. Res. Lett.*, **44**, 4332–4340, https://doi.org/10.1002/2017GL072843.

Zhang, Y., Y. J. Zhang, D. Zheng, and W. T. Lu, 2018c: Characteristics and discharge processes of M events with large current in triggered lightning. *Radio Sci.*, **53**, 974–985, https://doi.org/10.1029/2018RS006552.

Zhang, Y. J., S. D. Chen, D. Zheng, W. T. Lu, and B. Li, 2013a: Experiments on lightning protection for automatic weather stations using artificially triggered lightning. *IEEJ Transactions on Electrical and Electronic Engineering*, **8**, 313–321, https://doi.org/10.1002/tee.21861.

Zhang, Y. J., and Coauthors, 2014c: Experiments of artificially triggered lightning and its application in Conghua, Guangdong, China. *Atmospheric Research*, **135–136**, 330–343, https://doi.org/10.1016/j.atmosres.2013.02.010.

Zhang, Y. J., and Coauthors, 2016b: A review of advances in lightning observations during the past decade in Guangdong, China. *Journal of Meteorological Research*, **30**(5), 800–819, https://doi.org/10.1007/s13351-016-6928-7.

Zhang, Z. X., D. Zheng, Y. J. Zhang, and G. P. Lu, 2017e: Spatial-temporal characteristics of lightning flash size in a supercell storm. *Atmospheric Research*, **197**, 201–210, https://doi.org/10.1016/j.atmosres.2017.06.029.

Zhao, P. G., Y. Yin, and H. Xiao, 2015: The effects of aerosol on development of thunderstorm electrification: A numerical study. *Atmospheric Research*, **153**, 376–391, https://doi.org/10.1016/j.atmosres.2014.09.011.

Zhao, Y., X. S. Qie, M. L. Chen, X. Z. Kong, G. S. Zhang, T. Zhang, T. L. Zhang, and G. L. Feng, 2011: Characteristic of *M*-component in artificially-initiated triggered lightning. *Plateau Meteorology*, **30**(2), 508–517. (in Chinese with English abstract)

Zheng, D., Y. J. Zhang, Q. Meng, W. T. Lu, and X. Y. Yi, 2009: Total lightning characteristics and electric structure evolution in a hailstorm. *Acta Meteorologica Sinica*, **23**(2), 233–249.

Zheng, D., Y. J. Zhang, W. T. Lu, Y. Zhang, W. S. Dong, S. D. Chen, and J. R. Dan, 2012: Optical and electrical observations of an abnormal triggered lightning event with two upward propagations. *Acta Meteorologica Sinica*, **26**(4), 529–540, https://doi.org/10.1007/s13351-012-0411-x.

Zheng, D., Y. J. Zhang, W. T. Lu, Y. Zhang, W. S. Dong, S. D. Chen, and J. R. Dan, 2013: Characteristics of return stroke currents of classical and altitude triggered lightning in GCOELD in China. *Atmospheric Research*, **129–130**, 67–78, https://doi.org/10.1016/j.atmosres.2012.11.009.

Zheng, D., Y. J. Zhang, Q. Meng, L. W. Chen, and J. R. Dan, 2016a: Climatology of lightning activity in South China and its relationships to precipitation and convective available potential energy. *Adv. Atmos. Sci.*, **33**(3), 365–376, https://doi.org/10.1007/s00376-015-5124-5.

Zheng, D., Y. J. Zhang, Q. Meng, L. W. Chen, and J. R. Dan, 2016b: Climatological comparison of small- and large-current cloud-to-ground lightning flashes over Southern China. *J. Climate*, **29**, 2831–2848, https://doi.org/10.1175/JCLI-D-15-0386.1.

Zheng, D., and Coauthors, 2017: Characteristics of the initial stage and return stroke currents of rocket-triggered lightning flashes in southern China. *J. Geophys. Res.*, **122**, 6431–6452, https://doi.org/10.1002/2016JD026235.

Zheng, T. X., G. P. Lu, Y. B. Tan, Y. F. Fan, R. B. Jiang, H. B. Zhang, M. Y. Liu, and X. S. Qie, 2018: Observation and analysis of polarity reversal for the burst-type magnetic pulses during the propagation of upward positive leader in rocket-triggered lightning. *Chinese Journal of Atmospheric Sciences*, **42**(1), 124–133, https://doi.org/10.3878/j.issn.1006-9895.1705.17114. (in Chinese with English abstract)

Zhou, E. W., W. T. Lu, Y. Zhang, B. Y. Zhu, D. Zheng, and Y. J. Zhang, 2013: Correlation analysis between the channel current and luminosity of initial continuous and continuing current processes in an artificially triggered lightning flash. *Atmospheric Research*, **129–130**, 79–89, https://doi.org/10.1016/j.atmosres.2012.10.020.

Zhu, B. Y., H. L. Zhou, R. Thottappillil, and V. A. Rakov, 2014: Simultaneous observations of electric field changes, wideband magnetic field pulses, and VHF emissions associated with K processes in lightning discharges. *J. Geophys. Res.*, **119**, 2699–2710, https://doi.org/10.1002/2013JD021006.

Zhu, B. Y., M. Ma, W. W. Xu, and D. Ma, 2015: Some properties of negative cloud-to-ground flashes from observations of a local thunderstorm based on accurate-stroke-count studies. *Journal of Atmospheric and Solar-Terrestrial Physics*, **136**, 16–22, https://doi.org/10.1016/j.jastp.2015.07.007.

Zhu, R. P., T. Yuan, W. L. Li, and G. W. Na, 2013: Characteristics of global lightning activities based on satellite observations. *Climatic and Environmental Research*, **18**(5), 639–650, https://doi.org/10.3878/j.issn.1006-9585.2012.12017. (in Chinese with English abstract)